Chemistry
A European
Journal

Chemistry Europe
European Chemical Societies Publishing

Accepted Article

Title: Review The overview of N-rich antennae investigated in lanthanide-based temperature sensing

Authors: Chris Victor Stevens, Flore Vanden Bussche, Anna M. Kaczmarek, Véronique Van Speybroeck, Pascal Van Der Voort, Veronique Van Speybroeck, and Christian V. Stevens

To be cited as: *Chem. Eur. J.* 10.1002/chem.202100007

Link to VoR: https://doi.org/10.1002/chem.202100007

WILEY-VCH

10.1002/chem.202100007

Review

The overview of N-rich antennae investigated in lanthanide-based temperature sensing

Flore Vanden Bussche[a,b], Anna M. Kaczmarek[b], Veronique Van Speybroeck[c], Pascal Van Der Voort[b], Christian V. Stevens[a]

[a] ir. Flore Vanden Bussche, Prof. Dr. ir. Christian V. Stevens
Department of Green Chemistry and Technology
Ghent University
Email: Chris.Stevens@ugent.be
[b] Prof. Dr. Anna M. Kaczmarek, ir. Flore Vanden Bussche, Prof. Dr. Pascal Van Der Voort
Department of Chemistry
Ghent University
Krijgslaan 281 (S3), 9000, Ghent, Belgium
[b] Prof. Dr. ir Veronique Van Speybroeck
Department of Applied Physics
Ghent University
Technologiepark 46, 9052, Zwijnaarde, Belgium

Abstract

The market share of noncontact temperature sensors is expending due to fast technological and medical evolutions. In the wide variety of noncontact sensors, lanthanide-based temperature sensors stand out. They benefit from high photostability, relatively long decay times and high quantum yields. To circumvent their low molar light absorption, the incorporation of a light-harvesting antenna is required. This review provides an overview of the nitrogen-rich antennae in lanthanide-based temperature sensors, emitting in the visible light spectrum, and discuss their temperature sensor ability. The N-rich ligands are incorporated in many different platforms. The investigation of different antennae is required to develop temperature sensors with diverse optical properties and to create a diverse offer for the multiple application fields. First the molecular probes, consisting of small molecules, are discussed. Furthermore, the thermometer properties of ratiometric temperature sensors, based on di- and polynuclear complexes, metal-organic-frameworks, periodic mesoporous organosilicas and porous organic polymers, are summarized. The antenna mainly determines the application potential of the ratiometric thermometer. It can be observed that molecular probes are operational in the broad physiological range, metal-organic-frameworks are generally very useful in the cryogenic region, periodic mesoporous organosilica show temperature dependency in the physiological range and porous organic polymers are operative in the cryogenic to medium temperature range.

Introduction

The history of temperature sensing goes back to the Renaissance. From then on, measuring the temperature has challenged many great minds, from Galileo Galilei to Daniel Gabriel Fahrenheit and Andres Celsius.[1] Temperature affects nearly all biological and engineered systems.[2] Thermometers are therefore required in countless scientific and industrial environments, such as chemicals, oil and gas, consumer electronics, energy and power, automotive, healthcare, food and beverages, metals and mining, aerospace and defence, glass, and pulp and paper.[3-7] Their market share is depicted in Figure 1.[8] The temperature sensor market is expected to grow from USD 6.3 billion in 2020 to USD 8.8 billion by 2027, as recently projected in a market analysis by Markets and Markets.[8] Thermometers are subdivided into different categories. A distinction is based on the level of contact between sample and sensor; invasive sensors are in direct contact with the sample and non-invasive sensors measure the temperature remotely.[9] This review focuses on the latter, since their growth potential is tremendous,

10.1002/chem.202100007

based on the current device miniaturization, fast technological developments and advanced healthcare equipment.[8] In these domains, contact is impossible due to the scale of the sample, fast movement or inaccessibility of the object. Temperature gradients are visualised in for example photonic devices, microfluidics, micro-electronics, catalytic processes, and internal parts of combustion engines.[10-15] The application potential in the medicinal fields covers for instance in vivo thermal imaging and early tumor detection.[16-21] Current noncontact techniques are for example infrared thermography, thermoreflectance and thermographic phosphor luminescence. The infrared temperature sensors and fiber-optic temperature sensors are currently the main industrial applied non-contact thermometers. The thermographic phosphor luminescence is the upcoming and most promising accurate technique and is based on the thermal reading through phosphor light emission. Luminescent thermal sensors are derived from e.g. organic dyes, ruthenium complexes, polymers, quantum dots (QDs) and materials doped with lanthanide ions. The QDs and materials doped with lanthanide ions benefit from higher photostability. Since QDs generally include highly toxic elements (e.g. Cd), the main focus involves lanthanide-based materials showing temperature dependent luminescence.[9, 22-25] Different platforms are used in the design of lanthanide-based materials, such as metal organic frameworks, inorganic materials (phosphors and nanocrystals), inorganic-organic materials (coordination polymers, mesoporous silica).

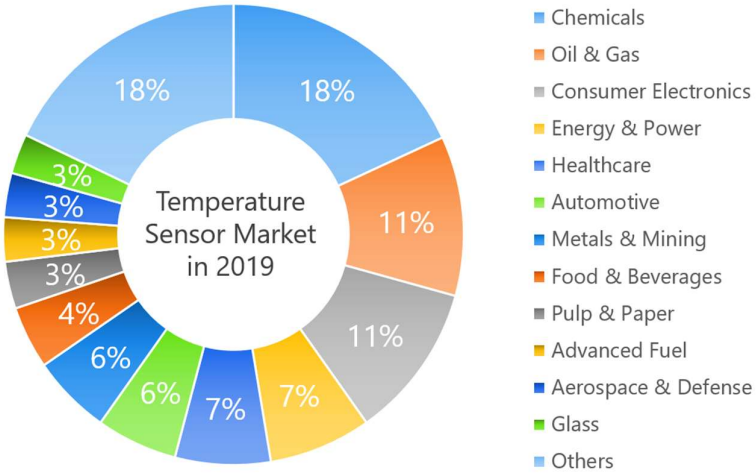

Figure 1. Overview of end-user industries for the temperature sensor market in 2019, valued at USD 6,043 million. 'Others' include HVAC, water & wastewater management, cement, telecommunications and agriculture. Figure adapted from reference. [8]

The importance of the lanthanides

Trivalent lanthanide ions (Ln^{3+}) absorb and emit electromagnetic radiation in the entire electromagnetic spectrum.[26-27] These ions are stable and narrow band emitters. The remarkable optical properties of lanthanide ions arise from partial filling of their 4f orbitals.[28-30] The electrons in this orbital are shielded by the filled 5s and 5p orbitals, since these appear further from the nucleus than the 4f orbital. They therefore do not overlap with ligand orbitals. The shielding implies spectroscopic and magnetic properties that are largely unaffected by the environment. The luminescence of trivalent lanthanides arises from 4f-4f transitions, and since these are shielded, the emission bands are narrow and well defined. Moreover, lanthanide ions have relatively long decay times, high quantum yields and high photostability. The 4f-4f transitions are however principally forbidden, resulting in inefficient excitation of the Ln^{3+} ion and thus low absorption coefficients. To circumvent this drawback, organic

10.1002/chem.202100007

ligands, which have allowed absorption transitions, are incorporated as antennae to capture the energy and transfer it to the lanthanides. This principle is known as 'the antenna effect' and is illustrated in Figure 2.[31]

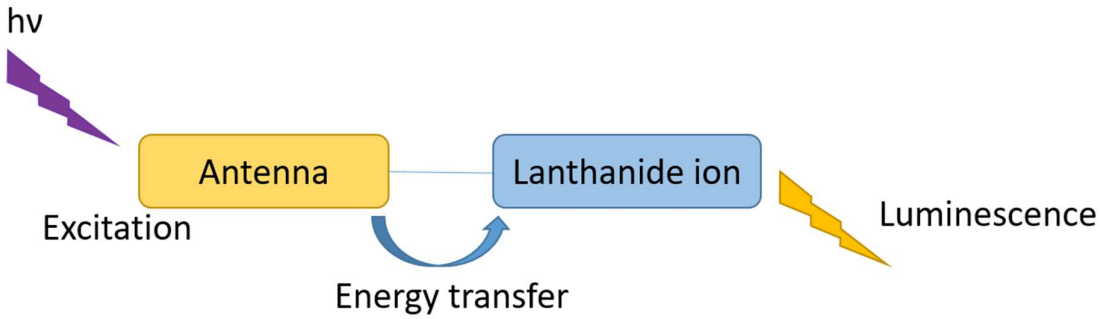

Figure 2. Simplified illustration of lanthanide based luminescence.

In this process first the ligand absorbs energy and undergoes transition from its singlet ground state S_0 to an excited S_1 state; second, the singlet S_1 state can transfer energy to the triplet T_1 state, via intersystem crossing (ISC). Third, the energy from the ligand is transferred to the lanthanide excited states, known as energy transfer. Lastly (and in the ideal scenario), radiative (light) emission occurs as the luminescent energy level relaxes back to lower lying (ground) state. The larger the energy gap between the lanthanide's emitting level and its highest lower lying energy level, the more intense luminescence will be. Furthermore, in order to have efficient energy transfer from the triplet state to the lanthanide ion, the energy of the triplet level should be closely matched with the Ln^{3+} accepting levels. The energy difference between T_1 of the ligand and the energy state of the lanthanide should therefore be about 2000 – 4000 cm^{-1}.[32] The temperature dependent luminescence originates from the balance between three possible pathways: i. thermal relaxation (vibrational relaxation of lanthanide ions), ii. energy transfer, related to the energy levels iii. energy back transfer from the lanthanide ion to the excited triplet state of the ligand (enhanced when their energy gap is less than 1850 cm^{-1}).[32-35] In the design of the lanthanide complex, selection of the lanthanide and the appropriate antennae is therefore crucial. Another incentive for the selection of the antenna, is the creation of a Lewis adduct.[36-37] The trivalent lanthanide ions are hard Lewis acids, the lanthanide complex will therefore preferentially interact with at least one Lewis base. N-donor ligands phenanthroline and bipyridine are popular bases since the resulting complex often shows intense luminescence. As an illustration, the luminescence and the emission spectra of $[Eu_x, Tb_{1-x}](L)$-bdc are shown in Figure 3.[38]

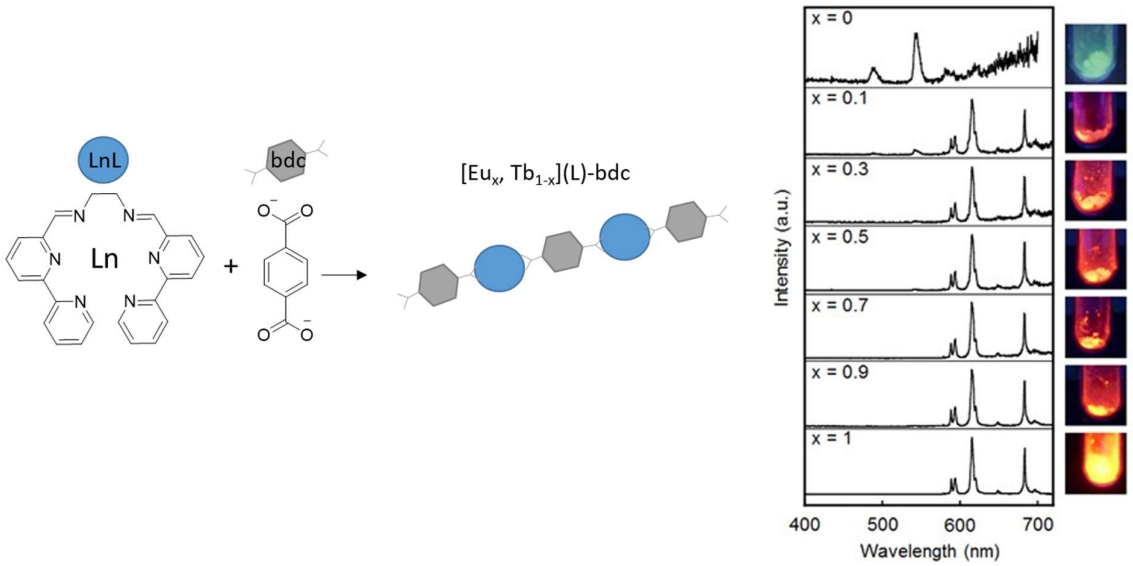

Figure 3. The emission spectra of [Eu$_x$, Tb$_{1-x}$](L)-bdc in the solid state at room temperature (excited at 315 nm), and the corresponding photographs of each solid sample showing the luminescence. [38] (Reprinted with permission from ref 38. Springer Nature, 2014)

Moreover, the extra Lewis base minimizes radiationless deactivation.[39] Furthermore, electronegative donor atoms are preferred in the trivalent lanthanide complex, with O-donors yielding the most effective coordination properties towards lanthanides. When looking at the literature, lanthanide β-diketonate complexes are the most popular, forming mostly 'tris' complexes with two coordination sites available for the neutral Lewis base ligand. Europium and terbium are the most widely studied luminescent lanthanide ions, since their energy level matches well with the triplet level of the reported N-rich ligands which feature intense luminescence, followed by dysprosium and samarium. These trivalent ions show emission in the visible light spectrum, however, near-infrared (NIR) emission is also observed. This review provides an overview of the N-donor antennae used in temperature sensing, consisting of these particular lanthanide ions, with the focus on resulting luminescent emission in the visible light spectrum. N-rich ligands have been incorporated in multiple platforms containing antennae ligands, ranging from porous materials as metal organic frameworks (MOFs), covalent organic frameworks (COFs), porous organic polymers (POPs) and periodic mesoporous organosilica (PMOs) over nonporous coordination polymers, small molecules and organic-inorganic hybrids.[23, 32, 39-47] The investigation of different antennae is required to develop temperature sensors with divers optical properties and to create a divers offer for the different application fields. Sensors are typically operative in a distinct temperature region, namely cryogenic (up to 100 K), medium (100 – 300 K), biological/physiological (298 – 323 K) and the high temperature region (≥ 450 K). This review provides an overview of the nitrogen-rich antennae used in the different material categories and discusses their corresponding temperature sensor ability. Previous reported reviews mostly focus on one category of material, thereby covering for example the MOFs, PMOs or small molecules.[32, 42-44, 47-48] With this review, we show that the base in the design of every temperature sensor is equal throughout all types of material, covering the conscious choice of the N-donor antennae and lanthanide ions when having the ultimate goal in mind. In the first part, lanthanide-based temperature sensors with N-rich antennae in small molecules will be discussed. These complexes merely depend on the emission intensity of a single transition, creating a system which can be affected by fluctuations of the measurement equipment. To avoid these fluctuations, sensors based on two transitions, known as ratiometric

temperature sensors, were developed. In the discussion of the ratiometric thermometers, a distinction is made between the following types of materials; di- and polynuclear complexes, metal-organic-frameworks, periodic mesoporous organosilicas and porous organic polymers.

Important performance parameters for temperature sensors

The performance of different lanthanide-based temperature sensors is assessed on five key parameters. These parameters are crucial for a quantitative comparison and evaluation of the developed thermometers. An in-depth review on these different parameters is recently conducted by Carlos and co-workers.[9] Here, we briefly summarise their most important features. The first parameter is the relative thermal sensitivity (S_r), indicating the relative change of the thermometric parameter Δ (Equation 1) per degree of temperature change (Equation 2, % K^{-1}). This valuable parameter is independent of the nature of the thermometer, allowing direct comparison of ratiometric thermometers over different categories of materials. The maximum value of Sr, S_m, at a certain temperature T_m is mostly reported. The second parameter is the temperature uncertainty (δT), also known as temperature resolution. It describes the smallest temperature change resolvable by the thermometer (Equation 3). This parameter depends on both the material and the experimental setup (f. ex. acquisition conditions, experimental detection setup, signal-to-noise ratio). The third parameter is the repeatability R, illustrating the ability of the thermometer to repeatedly provide the same result, under the same circumstances (Equation 4). The fourth and fifth parameters are resolution and reproducibility. The spatial δx and temporal δt resolutions are respectively the minimum resolvable distance or time interval between two measurements. The reproducibility is defined as the change of the same measurement, carried out under modified circumstances, such as different equipment, different measurement method, different operator.

Thermometric parameter Δ

$$\Delta = \frac{I1}{I2} \quad (1)$$

With I_1 and I_2 the integrated intensities of two transitions

Relative thermal sensitivity S_r

$$\mathrm{S}_r = 100\% \times \left|\frac{1}{\Delta}\frac{\partial \Delta}{\partial T}\right| \quad (2)$$

Temperature uncertainty δT

$$\delta \mathrm{T} = \frac{1}{S_r}\frac{\delta \Delta}{\Delta} \quad (3)$$

Repeatability R

$$\mathrm{R} = 1 - \frac{max|\Delta c - \Delta i|}{\Delta c} \quad (4)$$

With Δc the mean thermometric parameter and Δi the thermometric parameter measured at each temperature

The temperature will affect the luminescence of the discussed temperature sensors. The induced changes are monitored based on distinct parameters of the emitting center.[23] A distinction is made between i. the integrated emission intensity of a single transition or a pair of transitions ii. the spectral shift, polarization, or bandwidth of a certain transition iii. lifetime measurements, focusing on time-decay intensity profiles of the excited emitting states. As stated before, this review focusses first on small molecules with a single transition, thereby reporting the luminescence lifetime of the developed temperature sensors. Second, the focus is on ratiometric temperature sensors. Here, the measurement is based on the relative change in the intensity ratio of two independent energy-close transitions. The emission bands originate either from a single luminescent center, known as single-center thermometers, or from two distinct emitting centers, known as dual-center thermometers. The

dual center thermometers are more discussed in this review on organic based antennae, as dual type thermometers are more common in such materials. In inorganic nanoparticles, single center thermometers e.g. Nd^{3+} and Er^{3+} are very common.[6]

N-rich antennae incorporated in small molecules

The first group of compounds that will be discussed are the small molecule emissive probes. In these probes, one trivalent lanthanide ion is incorporated in the structure. The temperature sensors are characterised based on their luminescence lifetime τ, defined as the average time a molecule stays in the excited state.[49] This is calculated as the inverse of the sum of constants of radiative (k_r) and nonradiative (k_{nr}) processes.

$$\tau = \frac{1}{(\mathrm{kr} + \mathrm{knr})}$$

In 2003, Dalton et. al. synthesised a temperature sensitive paint, based on a tris(β-diketonate) phenanthroline europium(III) complex **1**.[50] The material showed temperature dependence over the temperature range 278 to 318 K, when dissolved in a polymer matrix. In the same year, Amao et al. incorporated tris(4,4,4-trifluoro-1-(2-thienyl)-1,3-butanediono)-1,10-phenanthroline europium(III) ($Eu(TTA)_3Phen$) **2** into poly(N-dodecylacrylamide) (PDDA) film, thereby creating a temperature sensitive sensor in the range of 320 - 370 K.[51] In 2004, Dalton et. al. incorporated complex **5** and **6** in a 1/600 dilution in fluoroacrylic polymer (FIB), creating a temperature sensitive paint in the temperature region 278 – 323 K.[39] In 2006, Wolfbeis et. al. developed three complexes **3**, including the dipyrazolyltriazine tris(β-diketonate) europium(III) complex **3a** ($Eu(TTA)_3(dpbt)$).[49] The dipyrazolyltriazine antenna allowed absorption in the visible light spectrum. Upon excitation at the ligand charge-transfer band (405 nm), their luminescence lifetime drastically decreased with increasing temperature. Furthermore, they dispersed the europium complex onto a poly(vinyl methyl ketone) (PVMK) film to improve the stability, after which temperature dependency was found between 274 K and 333 K. In 2008 and 2010, Stich et. al. successfully doped the europium(III) complex **3** into poly(vinyl chloride) (PVC) polymer to develop a temperature-sensitive-paint (TSP).[52-53] The TSP shows temperature dependency from 270 K to 310 K. In 2018 and 2020, Lapaev *et. al*. address the bottleneck of Eu^{3+}- based films: their moderate photostability. They developed more photostable temperature probes by using Eu(III) β-diketonate complexes **8, 9** with an anisometric geometry (i.e., the ratio of the long inertial axis of the molecule to its short inertial axis in the ellipsoid of revolution). Through the melt-processing technique, stable vitrified films are established from powders of the complexes. Complexes with longer alkyl chains undergo a glass transition with the formation of a vitrified, transparent and amorphous film, while shorter alkyl substituents crystallize and decompose upon heating.[54-56] An overview of different Eu^{3+}-containing temperature sensor complexes is given in Table 1. Two possible mechanisms are responsible for the temperature dependent behaviour of these europium-based complexes. The first is based on the thermal quenching process (nonradiative) from excited Eu(III) to vibrational relaxation.[57-58] The energy gap between the emitting level and the highest accepting level in 4f-4f transition of Eu^{3+} ions ($^5D_0$ - $^7F_6$: 12 297 cm^{-1}) is well-matched with the overtone of C-H and O-H vibrational frequencies, as depicted in Figure 4.[32] The coordination of water or other solvent molecules therefore potentially quenches the luminescence of the lanthanide ions. In a second mechanism, low-lying ligand-to-metal charge transfer states are responsible for the quenching of the thermal luminescence of Eu^{3+}-ions.[59] Overall, the europium-based probes are photoexcited in the 350 – 450 nm range and all probes are operational in the physiological temperature range.

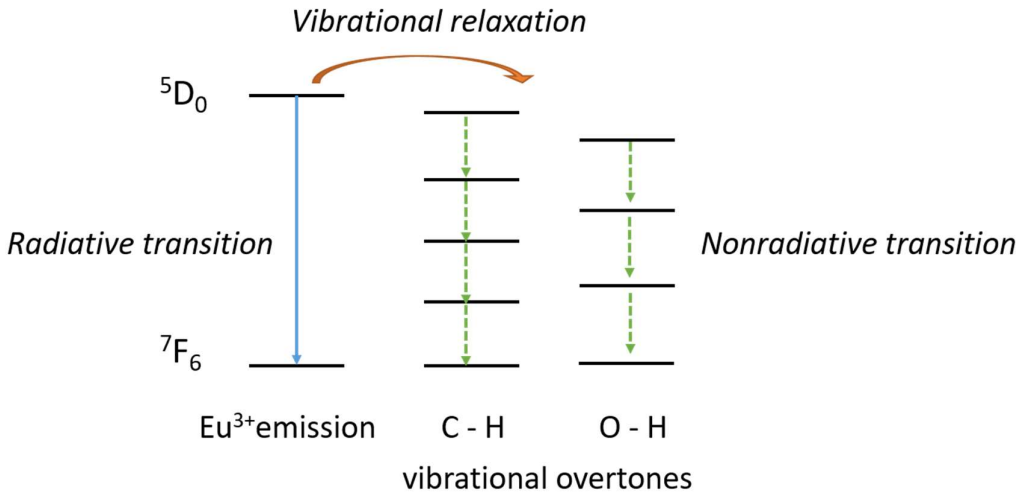

Figure 4. The vibrational overtones of C – H and O – H match the energy gap of the Eu(III) ion.

Next to europium, terbium based small molecules are designed as temperature sensor. The energy gap of Tb(III) ion ($^5D_4$ - $^7F_0$: 14 800 cm^{-1}) is larger than the energy gap of Eu(III) ions, the thermal quenching is therefore suppressed and temperature dependence is mainly determined by energy back transfer from the excited Tb(III) ions to the excited triplet state of the antenna.[32] Energy back transfer is enhanced if this energy gap is less than 1850 cm^{-1}.[34] An example of a terbium containing small molecule is developed by Lapaev *et.al*. in 2018.[60] The phenanthroline tris(1-(4-(4-propylcyclohexyl)-phenyl)decane-1,3-dionate (cpdk) Tb(III) complex (Tb(cpdk)$_3$(phen)) **8** shows temperature dependency in the region 143 - 253 K, after designing a film of the complex via a melt-processing technique. Furthermore, Brusso and co-workers coordinated the ligand 2-amidinopyridine (PyAm) to terbium and dysprosium (Ln(acac)$_3$(PyAm)).[61] The complexes show temperature-dependent changes in the thermal distribution of the Stark sublevels, showing different thermal populations within the same transition. At the supramolecular level, neighbouring mononuclear molecules interact through hydrogen bonding (illustrated in Figure 5). For the terbium complex, the lifetime value increased from 730 µs at 12.7 K to 829 µs at 320 K. For the dysprosium complex, the lifetime was reached at the detection limit of the equipment, which may impact the accuracy. An increase in lifetime was reported from 16.25 µs at 12.7 K to 18 µs at 320 K. The triplet level of PyAm was determined to be 26 500 cm^{-1}, thereby promoting efficient ligand to metal energy transfer. This was the first report experiencing such behaviour over a wide temperature range. The authors therefore stated further research was required to explain the observed increase in lifetime. Compared to the europium complexes, the terbium complex operates in a lower temperature region.

Table 1. Overview of the different N-rich antenna used in small molecule based temperature probes

Complex/Matrix	Temperature range (K)	Luminescence lifetime τ range (µs)	Ref.
1/PMMA	278 - 318	340 - 150	50
2/PDDA	320 - 370	N.D.*	51
3a/PVMK	274 - 333	500 – 190	49
3b/PVMK	274 - 333	455 – 150	49
3c/PVMK	274 - 333	625 – 240	49
3a/PVC	270 - 310	550 – 320	53
4/ PVDC-co-AN	278 - 328	N.D.*	62
5/FIB	278 - 323	350 – 80	39

10.1002/chem.202100007

6/FIB	278 - 323	400 – 110	39
7/PMMA	323 - 333	N.D.*	63
8/None	298 - 348	537 – 210	55
9/None	270 - 370	561 – 37	54
10/None	143 - 253	373 – 33	60
11(Tb)/None	18 - 320	730 - 829	61
11(Dy)/None	18 - 320	16 - 18	61

PMMA: poly(methyl methacrylate), PDDA: poly(N-dodecylacrylamide), PVMK: poly(vinyl methyl ketone), PVC: poly(vinyl chloride), PVDC-co-AN: poly (vinylidene chlorideco-acrylonitrile), FIB: fluoroacrylic polymer. *: The reported temperature dependency is based on temperature intensity.

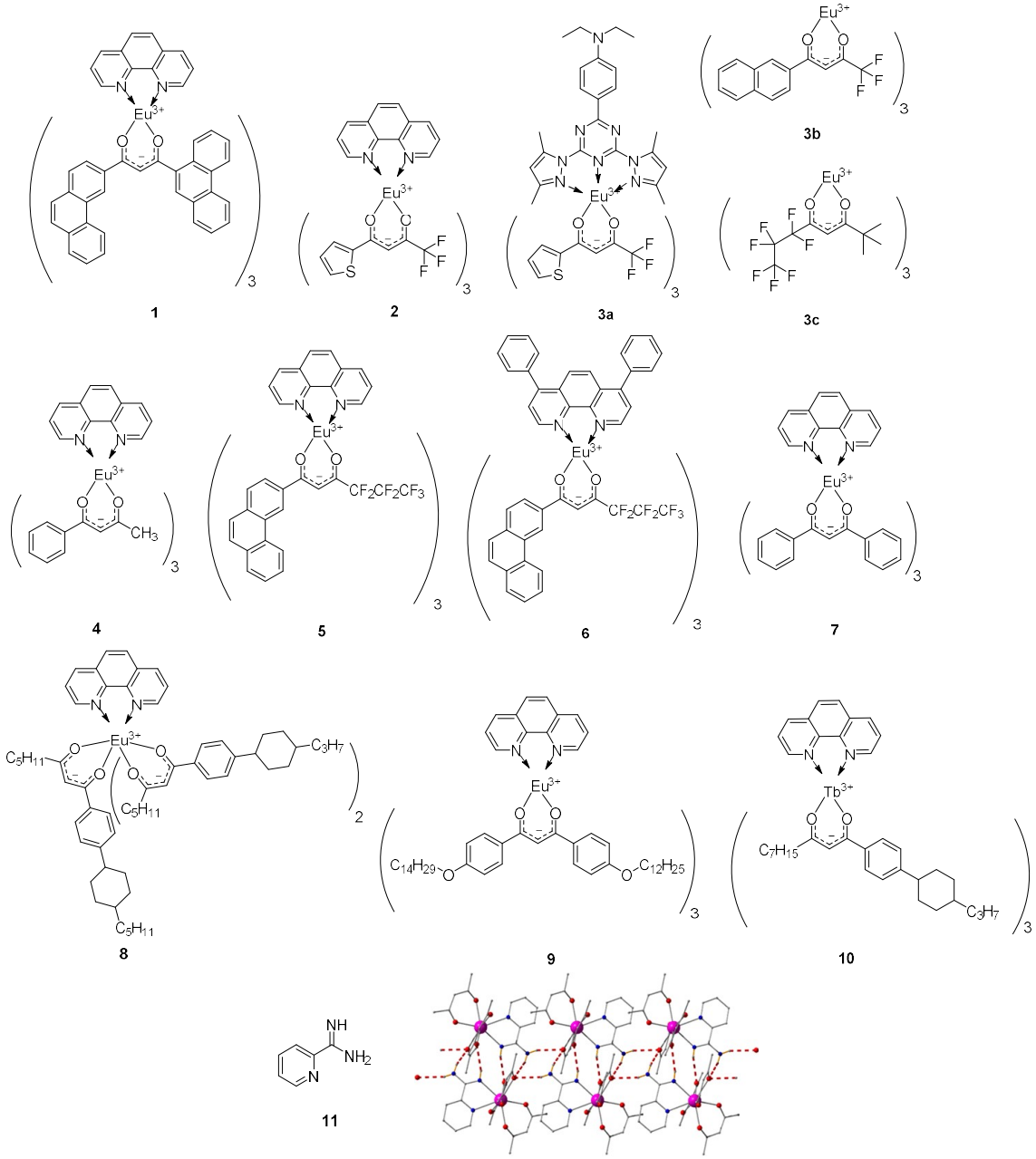

10.1002/chem.202100007

Figure 5. Overview of the Eu^{3+} and Tb^{3+} complexes with nitrogen rich antennae used in small molecule based temperature sensors.

The discussed small molecule-based temperature sensors are all mononuclear lanthanide complexes. In order to improve energy transfer, polynuclear lanthanide complexes are highly desirable. Swavey and co-workers designed two di-nuclear bipyrimidine Eu(III) β-diketonate complexes **11** and suggested electronic communication between the Eu^{3+}-ions via the bipyrimidine bridge, yielding a temperature sensor operative in the range 278 – 318 K.[64] The comparison of luminescent behaviour with the mononuclear bipyridine Eu(III) β-diketonate complexes **12, 13** did however not show any difference, implying little electronic communication. Murugesu and co-workers followed the same synthetic strategy.[65] They created three dinuclear terbium complexes, bridged by a planar 2,2´- bipyrimidine ligand. The remainder of the coordination environment is occupied by beta-diketonate ligands (acetylacetonate (acac), 1,1,1-trifluoroacetylacetonate (tfac), hexafluoroacetylacetone (hfac)). The complex with the acac- and the tfac-ligands shows temperature dependency in the temperature range 80 – 260 K, with a decrease in luminescence lifetime of 960 – 25 µs and 950 – 100 µs respectively. The hfac-based complex showed temperature dependency in the 80 – 323 K, with a decrease in luminescence lifetime from 960 – 350 µs. The T_1 energy of the ligands are approximately 24 800 (acac), 22 700 (tfac), 22 200 (hfac) and 23 350 (bpm) cm^{-1}. The sensitization mechanism therefore depends an efficient ligand-to-metal energy transfer of all the ligands involved.

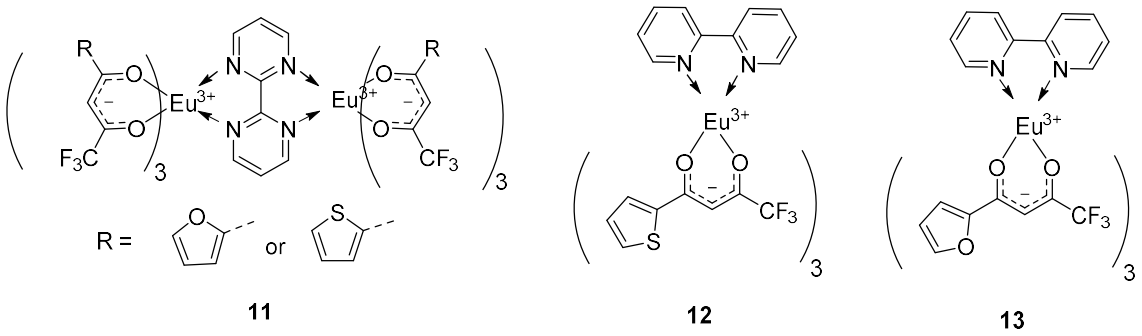

Figure 6. The temperature sensors developed by Swavey and co-workers.[64]

N-rich antennae incorporated in di- and polynuclear complexes

The discussed materials all depend on the emission intensity of a single transition, creating a system dependent on illumination fluctuations. The incorporation of different trivalent lanthanide ions allows its use as a ratiometric temperature sensor. A thermometer should therefore ideally have two discriminable emission peaks, in order to observe a clear luminescence and coherent temperature difference. The ratio of the two peaks eliminates fluctuations in (i) the excitation source (ii) the detector (iii) the concentration and inhomogeneity of the luminescent centers in the material. The ratiometric thermometers are subdivided in single center and dual center emissions. In a single center, the ratio arises from the emission transitions of two distinct transitions from the same emitting center, demonstrated in dysprosium-based sensors. However, Dy-based sensors are rare, since it is hard to find materials, which show strong Dy^{3+} luminescence due to the high energy accepting level of Dy^{3+} and the corresponding difficulty to find a matching triplet level. In a dual center, the ratio is calculated based on two different emitting centers, as specified in the introduction. The performance of different ratiometric thermometers in this review is compared using the following parameters: (i) temperature sensitivity, expressed in units of % change per degree of temperature change (% K^{-1}) (ii) temperature uncertainty (iii) repeatability and reproducibility. The temperature sensitivity, repeatability and reproducibility should be as high as possible, while the temperature uncertainty should not exceed 1 K. These different parameters have recently thoroughly been reviewed.[9]

10.1002/chem.202100007

A first example of a ratiometric thermometer is the luminescent organic polyhedra $Eu_{0.4}Tb_{3.6}$(triazole-pyridine-amido **14**)$_4$ developed by Sun and co-workers.[66] This soluble cage-like structure, depicted in Figure 7, shows temperature dependency in the region 200 – 360 K with a temperature sensitivity of 1.52 % K^{-1}. The energy gap between the triplet state of the ligand **14** (22 321 cm^{-1}) and the $^5D_4$ energy level of Tb^{3+}- ions (20 500 cm^{-1}) is smaller than 1850 cm^{-1}, implying energy back transfer from the excited Tb^{3+} state to the excited triplet state of the ligand. Secondly, Tanner *et. al*. developed a hetero-dinuclear Eu/Tb complex (cycEu-phTb **15**) active in the temperature region 10 – 200 K, with a temperature sensitivity of 1.86 % K^{-1}.[67] In 2018, Li and co-workers developed a flexible and transparent film through the solution casting method.[68] They cased a methanol solution of $Eu_{0.5}Tb_{0.5}$L (**16**) with a small amount of dimethylformamide solution of poly(methyl methacrylate) (PMMA), resulting in $Eu_{0.5}Tb_{0.5}$L@PMMA. The film showed temperature dependency in the range 77 – 297 K with a temperature sensitivity of 0.46 % K^{-1}. In 2019, Zhou *et al.* developed the complex $Tb_{1.95}Eu_{0.05}$pdc **17**, with the ligand pyridine-3,5-dicarboxylic acid (pdc).[69] The material is operative in the physiological range (298 – 318 K) with a maximum relative sensitivity of 0.64 % K^{-1}. The triplet excited state energy is 23 809 cm^{-1} and efficient ligand-to-metal energy transfer (LMET) to the Tb^{3+}-ions and subsequent energy transfer (ET) from Tb^{3+} to Eu^{3+} is observed. In 2019, Stevens and Van Der Voort reported a phenanthroline-based, insoluble polymer ($Tb_{0.5}Eu_{0.5}$_tfac@Phen-polymer **18**).[70] The material showed temperature dependency in the broad physiological range (260 – 460 K) with a maximum temperature sensitivity of 2.34 % K^{-1} at 340 K. The triplet excited state energy of the ligand is 24 096 cm^{-1}, the authors therefore assume the transfer of excitation energy from the phen-polymer to the $^5D_4$ accepting level of Tb^{3+} and subsequent transfer to the $^5D_0$ accepting levels of Eu^{3+}. Furthermore, the material showed repeatability up to 98 % and good temperature uncertainty ($\delta T < 1$) over the whole studied range.

10.1002/chem.202100007

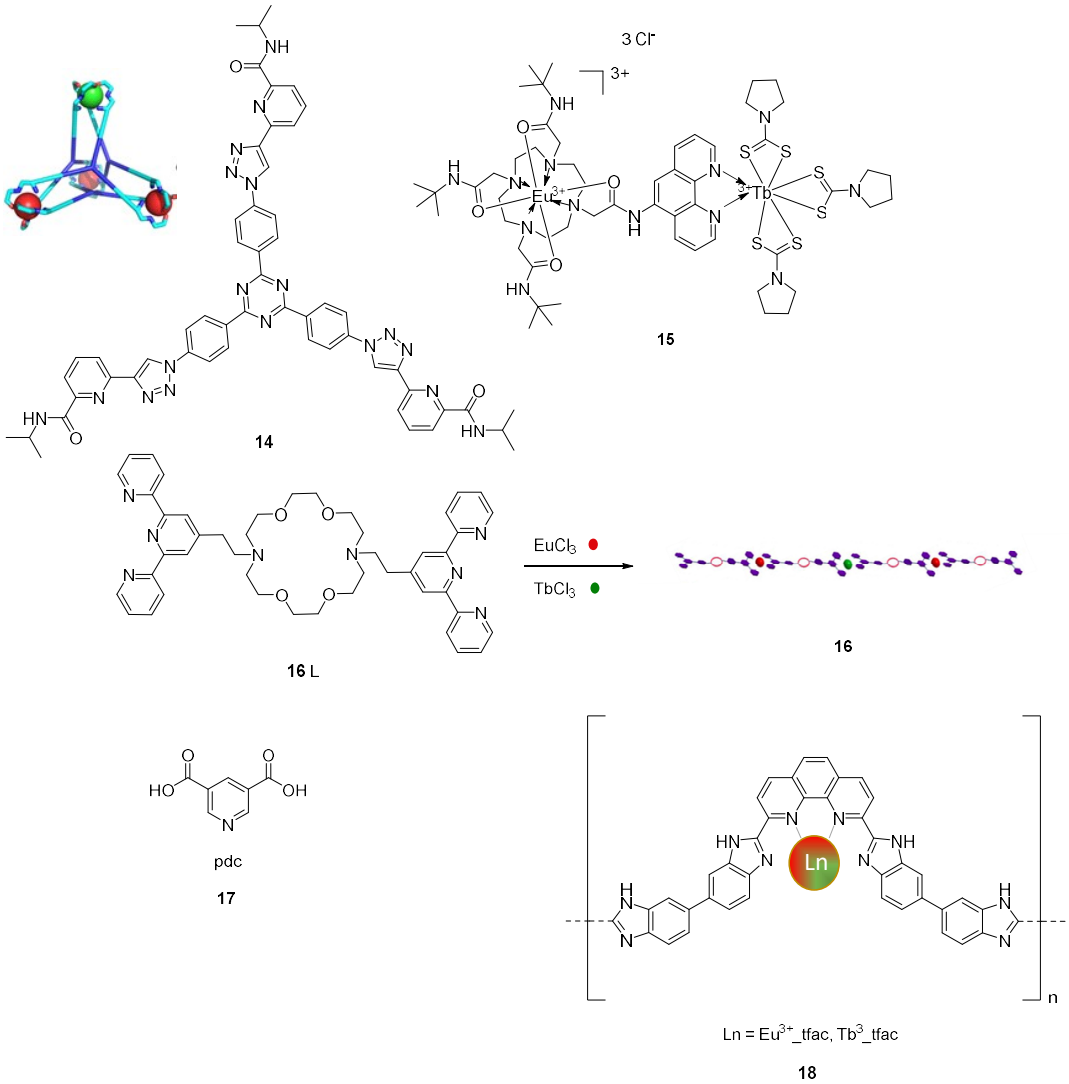

Figure 7. Polyhedra $Eu_{0.4}Tb_{3.6}$(triazole-pyridine-amido **14**)$_4$ developed by Sun and co-workers [66], the dinuclear cycEu-phTb complex **15** of Tanner *et. al.*[67], $Eu_{0.5}Tb_{0.5}$L (**16**) of Li and co-workers [68] and ligand **17** of the complex $Tb_{1.95}Eu_{0.05}$pdc [69], and $Tb_{0.5}Eu_{0.5}$_tfac@Phen-polymer **18** of Stevens and Van Der Voort.[70]

N-rich antennae incorporated in metal-organic-frameworks

Metal-organic-frameworks (MOFs) and coordination polymers are organic-inorganic hybrid materials with metal ions coordinated to organic ligand linkers. Variation in the metal ions and organic ligands allows the development of endless combinations, resulting in 1D, 2D or 3D structures. Their interesting luminescence properties arise from the metal ions, the ligands and the interactions between these building units. The creation of dual center emission MOFs proceeds via three routes, and is always based on the measurement of intensities of two transitions of distinct emitting centers (dual center). The first is based on a ligand (the organic linker) and a lanthanide ion, the second on two lanthanide ions (mostly Eu^{3+} and Tb^{3+}) and the third an a dye, hosted in the pores of the MOF, and a lanthanide ion.[41, 71] The MOF-based thermometers discussed in this review all belong to the second category. The presence of multiple luminescent centers creates tunable, ratiometric temperature sensors. The triplet excited state energy level of the organic ligand is ideally located in the range 22 000 – 27 000 cm^{-1}, in order to match the main energy accepting levels of Eu^{3+} ($^5D_1$: 19 031 cm^{-1}) and Tb^{3+} ($^5D_4$: 20 500 cm^{-1}). In 2012, the first Eu^{3+}/Tb^{3+} mixed metal-organic-framework was investigated by Cui and co-workers for

temperature sensing.[72] The bridging ligand is 2,5-dimethoxy-1,4-benzenedicarboxylate (dmbdc), with a triplet excited state energy of 23 306 cm^{-1}. The resulting MOF $Tb_{0.9931}Eu_{0.0069}$dmbdc **19** showed a maximum temperature sensitivity of 1.15 % K^{-1} at 200 K in the region 50 – 200 K. The incorporation of nitrogen-rich ligands followed rapidly. Higher sensitivities and wider temperature response rates could be achieved by manipulating the energy transfer process, via changing the triplet excited state energy of the organic linker. In a follow-up study by the same research group, the use of the ligand 5-(pyridine-4-yl) isophtalate (pia) **20**, with a higher triplet excited energy (26 455 cm^{-1}), resulted in a MOF-based thermometer $Tb_{0.9}Eu_{0.1}$pia with a temperature sensitivity of 3.53 % K^{-1} in the region 100 – 300 K.[73] They assign the increase in sensitivity to the increase in triplet level. However, the ratio of Eu^{3+} and Tb^{3+} present is different in the two samples. Increasing the amount of Tb^{3+} in the MOF, $Tb_{0.99}Eu_{0.01}$pia, resulted in a non-reliable luminescent temperature sensor. The comparison between different MOF-based temperature sensors is therefore complex. Later on, Cui and co-workers developed a MOF, $Tb_{0.957}Eu_{0.043}$cpda, consisting of an organic ligand (5-(4-carboxyphenyl)-2,6-pyridinedicarboxylic acid (cpda) **21**) with a triplet excited state energy of 27 027 cm^{-1}. The temperature sensor operates in the region 40 -300 K with a maximal sensitivity of 16 % K^{-1} (300 K), the wider temperature region and the higher sensitivity are ascribed to the high triplet level of the ligand.[74] Wang and co-workers designed a MOF with the linker 5-(4-(tetrazol-5-yl)phenyl) isophthalic acid (tpi) **22**, $Tb_{0.9122}Eu_{0.0878}$tpi.[75] The material showed temperature dependency in the region 75 – 250 K with a maximum sensitivity of 4.9 % K^{-1} at 250 K. The lanthanide ions are incorporated in the MOF either as metal node through direct synthesis or through post-synthetic functionalization of the organic ligand in the MOF. In 2014, Yan and co-workers investigated the effect of varying the metal node (M) in a mixed M, Ln-MOF. They started from the nanosized MOF In(OH)(bpydc) (bpydc = 2,2´-bipyridine-5,5´-dicarboxylic acid **23**) and incorporated Eu^{3+} and Tb^{3+} via post-functionalization.[76] The bipyridyl moieties serve as free Lewis basic coordination sites. The $Tb_{0.995}Eu_{0.005}$@In(OH)(bpydc) showed temperature dependency in the region 283 – 333 K with a maximum temperature sensitivity of 4.47 % K^{-1} at 333 K. Moreover, the reproducibility and repeatability of the material were tested and approved. The mechanism involves energy transfer from Tb^{3+} to Eu^{3+} and energy back transfer from the emitting level of Tb^{3+} to the excited triplet state of the bpydc ligand. The triplet excited state energy was however not determined. Furthermore, the research team analogously synthesized $Tb_{0.995}Eu_{0.005}$@MOF-253 (MOF-253 = Al(OH)(bpydc)) and $Tb_{0.995}Eu_{0.005}$@COMOC-4 (COMOC-4 = Ga(OH)(bpydc)) with temperature sensitivities of 2.54 % K^{-1} and 1.97 % K^{-1} respectively, in the same temperature region. This work proves the importance of the choice of the metal node, on top of the ligands and (the percentage of) lanthanide ions. Yan and co-workers further reported post-synthetic functionalization of the bpydc-UiO-67 MOF (Zr used as metal node) with chlorine salts of Eu^{3+} and Tb^{3+}, resulting in the nanocrystalline material $Tb_{0.005}Eu_{0.995}$@UiO-67-bpydc.[77] The sensor operates in the temperature region 100 – 300 K with a maximum temperature sensitivity of 0.5 % K^{-1}. However, they claim to have the highest reported temperature sensitivity of 47.98 % K^{-1}, overselling their results with a factor 100. Kaczmarek et al. used the MOF $[Tb_2(bpydc)_3(H_2O)_3]\cdot$nDMF as a platform and grafted β-diketonate complexes of Eu^{3+} onto the bipyridine linkers through post-synthetic functionalization.[78] The MOF selected in this work showed breathing behaviour in the structure. Removal of the DMF solvents would result in a structure transformation, and a nonporous material would be formed. Two sensors were developed by changing the percentage of added Eu^{3+}complexes, the sensor with 7.3 % Eu^{3+} showed temperature dependency in the range 200 - 325 K with a maximum relative sensitivity of 1.33 % K^{-1} (325 K), and the sensor with 3 % Eu^{3+} is operational from 225 – 375 K with a maximal sensitivity of 2.59 % K^{-1} (225 K). The lowest triplet energy excited state energy of bpydc is 21 505 cm^{-1}. They observe efficient energy transfer from the ligand to Tb^{3+}. Moreover, the same research group developed the rare Tb^{3+}/Sm^{3+} codoped MOF253, functionalized with different β-diketonate complexes (acac and tfac).[79] The material $Tb_{0.9}Sm_{0.1}$MOF253_acac showed temperature dependency in the region 250 – 410 K, with a maximum relative thermal sensitivity of 1.87 % K^{-1} (410 K). $Tb_{0.95}Sm_{0.05}$MOF253_tfac is active as thermometer in the same temperature region, with a maximum of 13.72 % K^{-1} (250 K). Wang *et al.* developed three MOF-based temperature sensors, operative from 40 to 300 K, with the ligand 1,3-bis(4-carboxyphenyl)imidazolium (bcpi) **24**: $Tb_{0.9}Eu_{0.1}$bcpi has a maximum relative sensitivity of 0.11 % K^{-1}

10.1002/chem.202100007

(300 K), $Tb_{0.8}Eu_{0.2}L$ of 0.15 % K^{-1} (300 K) and $Tb_{0.7}Eu_{0.3}L$ of 0.17 % K^{-1} (300 K).[80] In 2018, Qian and co-workers designed the MOF $Tb_{0.81}Eu_{0.19}$pddi (pddi: 5,5′-(pyridine-2,5-diyl)diisophthalic acid **25**) with a maximum sensitivity of 0.37 % K^{-1} at 473 K, over the range 313 – 473 K.[81] The temperature range is clearly smaller and higher than the normal reported ranges. Furthermore, the MOF sensor showed good thermostability and spectral repeatability. The sensitivities correspond with a temperature resolution of 0.11 – 0.05 K. According to the authors, the accurate resolution suggest potential for the use in microelectronic diagnosis, since the accuracy is good enough to observe fluctuations in circuit chips. In 2020, Wang et al. developed a MOF with the ligand 4-(2,4,6-tricarboxylphenyl)-4,2′:6′,4′′-terpyridine (tcptpy) **26**, $Tb_{0.897}Eu_{0.103}$tcptpy.[82] The material is operative in the range 305 – 340 K and showed a high maximum sensitivity of 8.41 % K^{-1} at 340 K. The calculated triplet excited state of the linker was 22 321 cm^{-1} and effective ligand-to-metal energy transfer was observed. The strategy of incorporating mixed ligands into a MOF was introduced by Wu *et al*., with the aim to investigate their influence on the temperature sensing properties. Wu and co-workers selected 2,4-(2,2′:6′,2′′-terpyridin-4′-yl)-benzenedisulfonic acid (dstp **27**) as the first ligand and implemented an ancillary ligand as oxalic acid (OA) or 1,4-benzene dicarboxylic acid (bdc **28**).[83] The ancillary ligands enhance the thermal stability of the MOF, creating a thermally stable MOF up to 653 K and 788 K, respectively. They have successfully developed two types of highly thermal stable and sensitive thermometers $[Tb_{0.98}Eu_{0.02}(OA)_{0.5}(dstp)]\cdot 3H_2O$ and $[Tb_{0.98}Eu_{0.02}(bdc)(dstp)]\cdot 3H_2O$. The first sensor operates in the 77 – 275 K region with a maximum temperature sensitivity of 2.4 % K^{-1} at 275 K, the second operates in the range of 125 – 250 K with 2.8 % K^{-1} at 225 K. The typical temperature dependent mechanism was proposed; light-harvesting via the DSTP ligand, with a large π-conjugated system, and efficient energy transfer from Tb^{3+} to Eu^{3+}. The higher sensitivity of the bdc **28** based MOF was attributed to a more efficient energy transfer from Tb^{3+} to Eu^{3+}. Furthermore, five other groups investigated the use of mixed ligands for temperature sensing. Yan *et al.* reported a MOF with biphenyl-4,4′-dicarboxylate (bpdc) **29** and adenine (ad) **30** Ad/$Tb_{0.999}Eu_{0.001}$/bpdc, resulting in a thermometer operational in the 100 – 300 K region with a relative sensitivity of 1.23 % K^{-1}.[84] The thermal stability was however not reported. Du and co-workers developed a MOF with the linkers D-camphoric acid (D-cam) **31** and 4,5-imidazole dicarboxylic acid (Himdc) **32**, $Eu_{0.7}Tb_{0.3}$(D-cam)$(Himdc)_2(H_2O)_2]_3$.[85] The temperature sensor operates with a sensitivity of 0.11 % K^{-1} at 450 K in the range of 100 – 450 K. The MOF shows high thermal stability, up to 690 K. Hu *et al*. designed a Eu/Tb (4:6) coordination polymer with the ligands 2-(2-sulfophenyl)-imidazol(4,5-f)(1,10)-phenanthroline (sip) **33** and glutaric acid.[86] The material showed good thermal stability, up to 700 K. The sensor operates in the region 50 – 225 K with a sensitivity of 0.68 % K^{-1}. Zareba and co-workers investigated two CP consisting both of phenanthroline and 1,3,5-benzenetricarboxylic acid (1,3,5-btc), the first MOF contains 0.88 % Eu and 22.87 % Tb (1Eu23Tb) and the second MOF contains 1.74 % Eu and 21.88 % Tb (2Eu22Tb).[87] Both sensors are active in the physiological 293 – 393 K range, 1Eu23Tb shows a relative sensitivity of 2.37 % K^{-1} and 2Eu22Tb of 2.71 % K^{-1}. At last, Liu and co-workers investigated the MOF $[Tb_{0.92}Eu_{0.08}pidc(ox)_{0.5}H_2O]\cdot 3H_2O$ with the ligand 2-pyridin-4-yl-4,5-imidazoledicarboxylic acid (pidc) **34** and the ancillary ligand sodium oxalate (ox).[88] The sensor operates in the region 303 – 473 K, with a maximum sensitivity of 0.6 % K^{-1} at 473 K. The MOF is thermally stable up to 673 K. The authors claim a temperature resolution of 0.012 K. This low value implies the use of a detector with a relative uncertainty in Δ ($\delta\Delta/\Delta$) of 0.0072 %. The current sensitive detectors (as the photomultiplier tube used in the cited paper) show $\delta\Delta/\Delta$ of 0.02 – 0.03 %, making the reported temperature resolution of 0.012 K doubtful.[9, 81] A low temperature resolution suggests the MOF is accurate enough to monitor the temperature changes in pathological and normal cells. The cytotoxicity (via MTT assay, a colorimetric assay for measuring the activity of enzymes that are capable of reducing the dye compound MTT (3-(4,5-dimethylthiazol-2-yl)-2,5-diphenyltetrazolium bromide)) and biocompatibility (stability in phosphate-buffered saline solution for 24 h) of the MOF is therefore tested and approved.

10.1002/chem.202100007

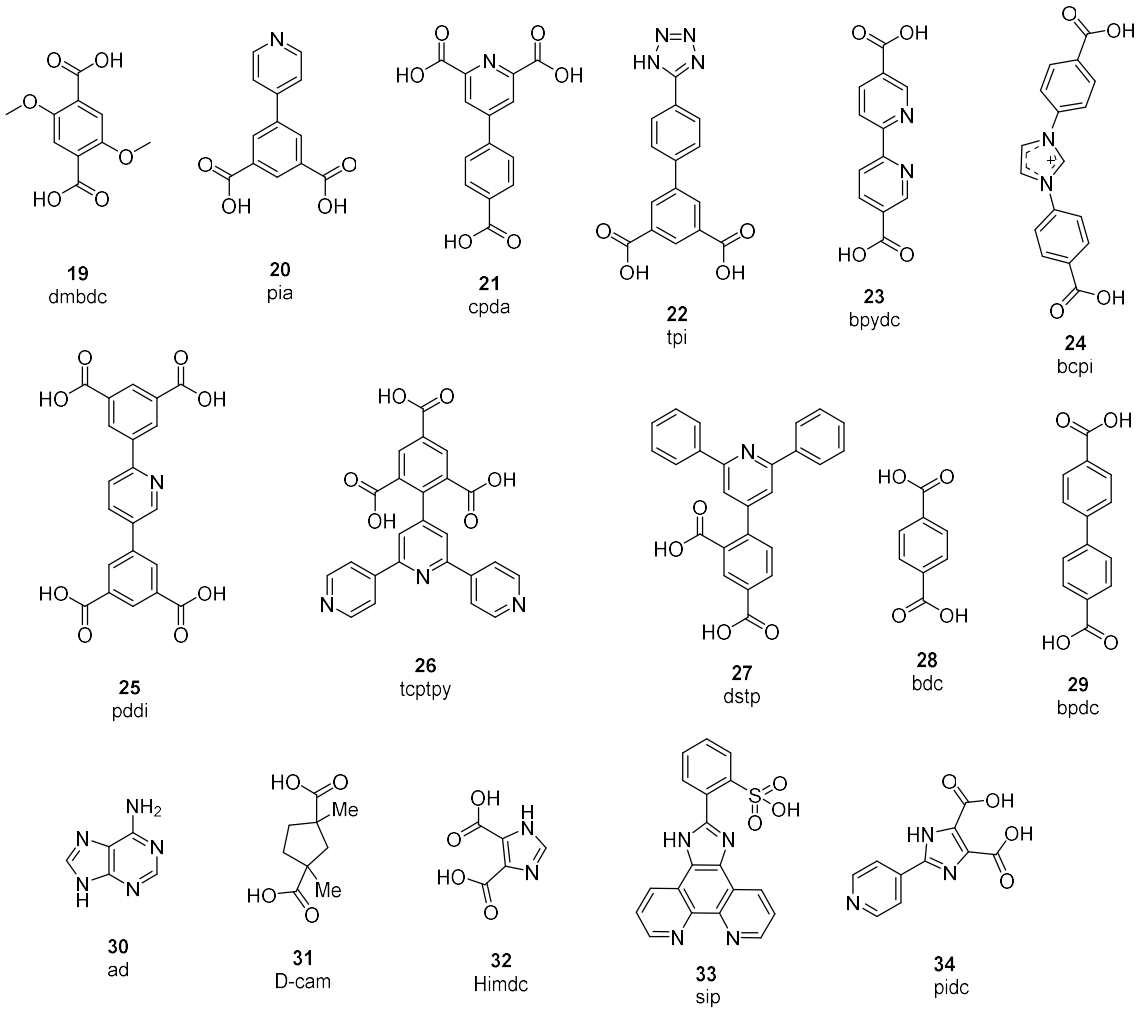

Figure 8. Overview of the N-rich antennae incorporated in metal-organic-frameworks for temperature sensing.

Table 2. Overview of the different N-rich antennae used in MOF-based temperature sensors

MOF	Temperature range (K)	S_m (% K^{-1}) at T_m (K)	Triplet level antenna (cm^{-1})	Ref
$Tb_{0.9931}Eu_{0.0069}$dmbdc **19**	50 – 200	1.15 (200)	23 306	[72]
$Tb_{0.9}Eu_{0.1}$pia **20**	100 – 300	3.53	26 455	[73]
$Tb_{0.957}Eu_{0.043}$cpda **21**	40 - 300	16 (300)	27 027	[74]
$Tb_{0.9122}Eu_{0.0878}$tpi **22**	75 – 250	4.9 (250)	21 505	[75]
$Tb_{0.995}Eu_{0.005}$@In(OH)(bpydc) **23**	283 – 333	4.47 (333)	21 505	[76]
$Tb_{0.995}Eu_{0.005}$@MOF-253 **23**	283 – 333	2.54	21 505	[76]
$Tb_{0.995}Eu_{0.005}$@COMOC-4 **23**	283 – 333	1.97	21 505	[76]
$Tb_{0.005}Eu_{0.995}$@UiO-67-bpydc **23**	100 - 300	0.5	21 505	[77]
TbMOF@7.3%Eu_tfac **23**	200 - 325	1.33 (325)	21 505	[78]
TbMOF@3%Eu_tfac **23**	225 - 375	2.59 (225)	21 505	[78]
$Tb_{0.9}Sm_{0.1}$MOF253_acac **23**	250 - 410	1.87 (410)	21 505	[79]
$Tb_{0.95}Sm_{0.05}$MOF253_tfac	250 - 410	13.72 (250)	21 505	[79]
$Tb_{0.9}Eu_{0.1}$bcpi **24**	40 - 300	0.11 (300)	ND	[80]
$Tb_{0.8}Eu_{0.2}$bcpi **24**	40 - 300	0.15 (300)	ND	[80]

$Tb_{0.7}Eu_{0.3}$ bcpi **24**	40 - 300	0.17 (300)	ND	[80]
$Tb_{0.81}Eu_{0.19}$pddi **25**	313 - 473	0.37 (473)	ND	[81]
$Tb_{0.897}Eu_{0.103}$tcptpy **26**	305 - 340	8.41 (340)	22 321	[82]
$[Tb_{0.98}Eu_{0.02}(OA)_{0.5}(dstp)]\cdot 3H_2O$ **27**	77 - 275	2.4 (275)	ND	[83]
$[Tb_{0.98}Eu_{0.02}(bdc)(dstp)]\cdot 3H_2O$ **27 28**	125 - 250	2.8 (225)	ND	[83]
Ad/$Tb_{0.999}Eu_{0.001}$/bpdc **29**	100 - 300	1.23	ND	[84]
$Eu_{0.7}Tb_{0.3}(D\text{-cam})(Himdc)_2(H_2O)_2]_3$ **31 32**	100 - 450	0.11 (450)	ND	[85]
$[Eu:Tb(4:6)sip(glu)]_n\cdot 2nH_2O$ **33**	50 - 225	0.68	ND	[86]
$[Tb_{0.92}Eu_{0.08}pidc(ox)_{0.5}H_2O]\cdot 3H_2O$ **34**	303 - 473	0.6 (473)	ND	[88]

Table 2 provides an overview on the discussed temperature sensors. The relative temperature sensitivity is influenced by multiple factors. First, the lanthanide ions present and the ratio of these lanthanides is decisive. A large excess of the terbium ions over europium or samarium ions provides the best result. Next, the triplet level of the N-rich antenna plays a role. The highest reported sensitivity for the N-rich MOFs corresponds to the ligand with the highest triplet level. Third, the influence of the other ligands present in the lanthanide complex determine the outcome. This can clearly be seen from the influence of the β-diketones tfac and acac in the Tb/Sm based MOF. To put this table in perspective, the highest reported relative temperature sensitivity in MOFs is 31 % K^{-1} (4 K) in the temperature region 4 – 50 K, obtained in the mixed-metal MOF $Tb_{0.95}Eu_{0.05}HL$ (H_4L: 5-hydroxy-1,2,4-benzenetricarboxylic acid).[89] The triplet level of the ligand is estimated to be 26 600 cm^{-1}. The energy difference between the triplet state of the ligand and the Tb^{3+} emitting level ($^5D_4$, 20 500 cm^{-1}) is approximately 6100 cm^{-1}, the energy can thus be transferred without significant energy back transfer. The MOFs generally operate in a broad temperature region, focussing on the physiological and cryogenic range. Their application potential therefore covers for example biological thermometers and the aerospace industry and superconducting magnets.[90] Higher temperatures are often not reported due to the thermal instability of these materials.

N-rich antennae incorporated in periodic mesoporous organosilicas

The following category of materials that will be discussed is the periodic mesoporous organosilicas (PMOs). PMOs are prepared through polycondensation of silica containing organic linkers around a template, and after removal of the template, a well-ordered mesoporous structure remains. Incorporating linkers with binding sites for lanthanide complexes recently gained attention. In 2018, the first report on the DPA PMO for visible light temperature sensing appeared. Kaczmarek et al. synthesised a PMO starting from 5 % N,N-bis(trimethoxysilylpropyl)-2,6-pyridine dicarboxamide (dpa) **35** and 95% tetraethyl orthosilicate, and grafted different ratios of Tb^{3+}/Eu^{3+} and Tb^{3+}/Sm^{3+} chloride salts onto the material.[91] To enhance the luminescence, 1,10-phenanthroline was added as a co-ligand in the grafting process. The Tb^{3+}/Eu^{3+} grafted PMO nanoparticles showed temperature dependent behaviour in the region 260 – 460 K. $Eu_{0.25}Tb_{0.75}$DPA-PMO has a maximum relative sensitivity of 1.22 % K^{-1} (440 K), $Eu_{0.50}Tb_{0.50}$DPA-PMO a maximum of 1.56 % K^{-1} (360 K) and $Eu_{0.75}Tb_{0.25}$DPA-PMO a maximum of 1.45 % K^{-1} (340 K). The authors observe energy transfer from Tb^{3+} to Eu^{3+}, suggesting that they graft closely together onto the PMO framework. As can be seen, a specific choice of the lanthanide ratio is important. The sensor $Sm_{0.95}Tb_{0.05}$DPA-PMO is operational in the region 280 – 460 K with a maximum relative sensitivity of 2.38 % K^{-1} (340 K). Energy transfer from Tb^{3+} to Sm^{3+} is observed based on the changing decay times over the temperature interval. Obtaining strong Sm^{3+} emission (especially at elevated temperature) is difficult, therefore, Tb^{3+}/Sm^{3+} based sensors are rare. All these sensors are operational in the broad physiological range, moreover PMOs are known for their high

10.1002/chem.202100007

biocompatibility, making them attractive, potential biological nanothermometers.[42] In 2019, Jena, Kaczmarek and co-workers coupled picolinic acid onto a monoallyl ring PMO via thiol-ene click chemistry.[92] Afterwards, equal molar ratios of Eu^{3+} and Tb^{3+} ions were grafted onto the material resulting in $Eu_{0.5}Tb_{0.5}$@Pic@PMO **36**. The triplet level of the Pic@PMO was estimated around 25 252 cm^{-1}. The energy of the ligand is efficiently transferred from the ligand to the Tb^{3+} emitting level, and subsequent Tb-to-Eu energy transfer. This process proves close proximity of the lanthanide ions. The materials operates as a thermometer with a maximum relative sensitivity of 2.1078 % K^{-1} (273 K) in the physiological region (270 – 373 K). In 2020, Inagaki, Van Der Voort and co-workers developed Dy-Dy and Tb-Sm based bipyridine PMOs.[93] They investigated pure 2,2´-bipyridine PMO (bpy-PMO **37**) and a bipyridine-ethane co-condensed PMO (bpy-Et-PMO **38**). Grafting of $Dy(acac)_3$ complexes onto bpy-PMO, resulted in a sensor operational in the temperature region 200 – 400 K with a maximum relative sensitivity of 2.85 % K^{-1} (200 K). When $Dy(acac)_3$ complexes were grafted onto bpy-Et-PMO, a sensor with maximum sensitivity of 1.46 % K^{-1} (300 K) in the region 200 – 400 K was obtained. With temperature increase, the higher energy level of Dy^{3+} ($^4I_{15/2}$) becomes populated and, hence, its emission intensity increases gradually, at the expense of the population of the lower state ($^4F_{9/2}$). A ratiometric temperature sensor is established from the changing intensity ratio of these peaks. Furthermore, the authors investigated the thermometer potential when grafting multiple ratios of Tb^{3+}/Sm^{3+} onto the different PMOs. The bpyPMOs showed temperature dependency in the region 253 – 333 K, $Sm_{0.9}Tb_{0.1}(acac)_3$bpy-PMO with a maximum relative sensitivity as high as 4.93 % K^{-1} (253 K) and $Sm_{0.8}Tb_{0.2}(acac)_3$bpy-PMO a maximum of 4.82 % K^{-1} (253 K). The sensors based on bpy-Et-PMO are operational in the region 253 – 373 K, $Sm_{0.9}Tb_{0.1}(acac)_3$bpy-Et-PMO shows a maximum sensitivity of 3.83 % K^{-1} (323 K), $Sm_{0.8}Tb_{0.2}(acac)_3$bpy-Et-PMO a maximum of 3.72 % K^{-1} (323 K). The sensors consisting of pure bipyridine linkers are better thermometers, furthermore, a higher amount of Sm^{3+} over Tb^{3+} is beneficial. The (grafted) PMO materials were tested for their toxicity towards fibroblastic cells of normal human dermal fibroblasts, showing a complete absence of toxicity. Furthermore, the materials were tested in water, forming stable colloidal suspensions and showing very good thermometric properties. The investigated materials could therefore be promising candidates for biomedical temperature sensing, despite being excited and emitting in the visible region and not the NIR region, which is more favourable for biomedical temperature sensing due to deeper tissue penetration. They could be useful for example in the fundamental studies of the biological, biochemical and physiological processes happening in cells where visible light is suitable for use.

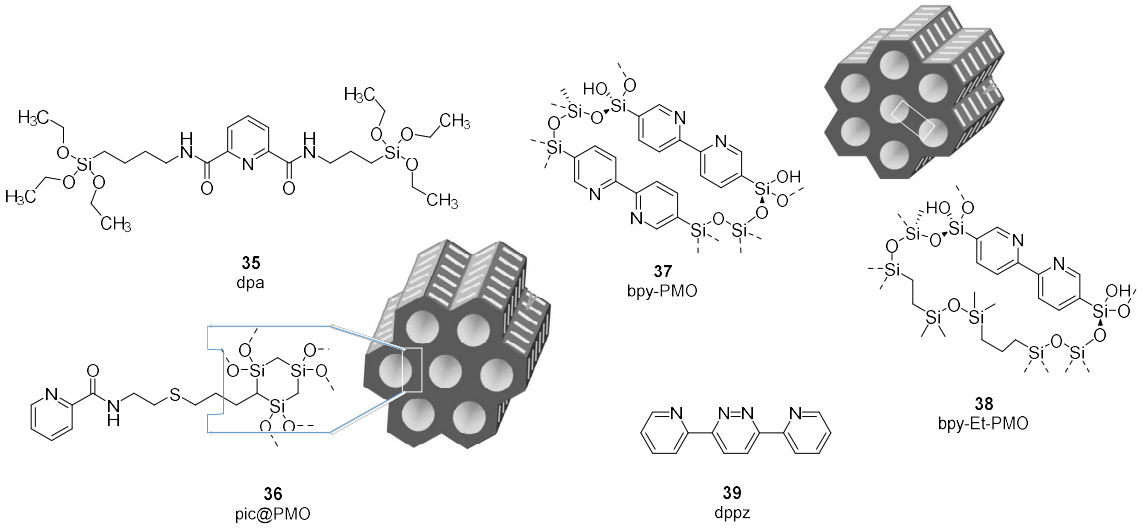

Figure 9. Reported lanthanide grafted PMO materials tested for temperature sensing.

Furthermore, a mesoporous silica (this material is not a PMO since its synthesis is conducted in the presence of a silica source (TEOS)) decorated with dipyridyl-pyridazine (dppz) **39** ligands and grafted with 28 % Eu^{3+} and 72 % Tb^{3+} ions was investigated by Kaczmarek and co-workers as a temperature sensor.[94] The material showed a maximum relative sensitivity of 1.32 % K^{-1} (260 K) over the range 10 – 360 K. The N-rich ligand dppz could also be used to prepare thermometers with NIR emitting lanthanides (Nd, Yb, Er).[95]

N-rich antennae incorporated in porous organic polymers

The fully organic counterpart of the metal-organic-framework, covalent organic framework (COF), consist purely of covalently bonded, organic building blocks. Varying the building blocks results in a wide library of potential crystalline, porous 2D or 3D frameworks. COFs benefit from high thermal and chemical stability, making them ideal candidates for temperature sensing. In light of the application, organic π-systems are preferred over their saturated counterparts, since these system are more prone to electronic excitations (lower energy difference for a π-π* transition than for a σ-σ* transition). Until now (June 2020), only one report investigates the use of COFs in temperature sensing. Kaczmarek and co-workers started from the imine-linked TpBpy-COF, prepared from 1,3,5,-triformylphloroglucinol (Tp) **40** and 2,2´-bipyridine-5,5´-diamine (Bpy) **41**, and grafted different ratios of Eu^{3+}/Tb^{3+} and Dy^{3+} acetylacetone complexes onto the framework.[96] The Eu^{3+}/Tb^{3+} based temperature sensors all operate in the broad temperature region 10 – 360 K. Varying the ratio of Eu^{3+}/Tb^{3+} provided insight in the ideal composition. $Eu_{0.6}Tb_{0.4}$@TpBpyCOF shows a maximum relative sensitivity of 1.018 % K^{-1} (160 K), $Eu_{0.8}Tb_{0.2}$@TpBpyCOF a maximum of 1.403 % K^{-1} (160 K) and $Eu_{0.95}Tb_{0.5}$@TpBpyCOF a maximum of 1.342 % K^{-1} (160 K). Remarkably, for all the sensors peculiar temperature dependent behaviour was observed; Tb^{3+} emission is namely not temperature dependent over the investigated range, as can be seen in Figure 10. This is related to the absence of energy back transfer from Tb^{3+} to the ligand, the energy of the lowest ligand triplet level (around 400 nm) is well above the $^5D_4$ acceptor level of Tb^{3+}. The excited Eu^{3+} levels (around 400 nm - 25 000 cm^{-1}) are however closer and allow metal-to-ligand back transfer, concomitantly decreasing the $^5D_0$ lifetime as temperature increases.[97] Furthermore, the phenomenon suggests no Tb^{3+} to Eu^{3+} energy transfer. This was studied in detail through monitoring the decay times over the temperature range, the decay time of Tb^{3+}indeed remained constant with increasing temperature. A second part of the manuscript focuses on $Dy(acac)_3$ grafted TpBpyCOF. The sensor operates in the region 280 – 440 K, with a maximum relative sensitivity of 0.942 % K^{-1} (280 K). The temperature uncertainty is below 0.05 K, confirming the good thermometer performance. The potential of COFs in temperature sensing is tremendous. The use of the antennae could for example be further explored through the creation of more stable linkages and increasing the effectiveness of π-conjugation.[47] Furthermore, different temperature regions, compared to the reported MOFs, and subsequent different applications could be investigated.

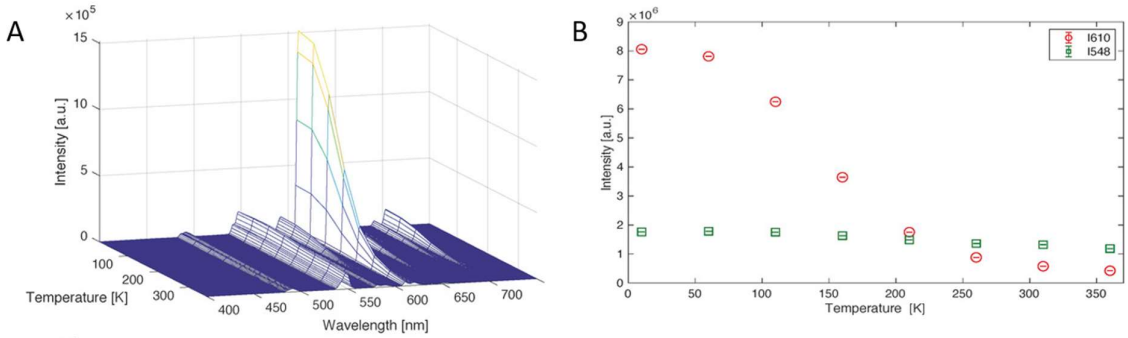

Figure 10. Plots for sample $Eu_{0.8}Tb_{0.2}$@TpBpyCOF. A shows the emission map recorded between 10 – 260 K and plot B the integrated-area values as a function of temperature. The green squares correlate to the 548 nm values, the red circles to the 610 nm values. The emission of Tb^{3+} (green squares) does not show temperature dependency. Reproduced with permission.[96]

So far, crystalline, porous materials were discussed as potential temperature sensor. Crystallinity was thought to have a crucial influence on the luminescent properties. The interactions between monomer units and adjacent layers are less understood in amorphous systems. Nevertheless, we found it interesting to investigate the potential of amorphous materials in temperature sensing. In 2020, Kaczmarek *et al.* were the first to explore an amorphous, porous organic polymer (POP) for temperature sensing. The starting materials are 6,6'-(2,2'-bipyridine-5,5'-diyl)bis(1,3,5-triazine-2,4-diamine) (bpyDAT) **42** and terephthalaldehyde **43**, creating an aminal connected framework. The framework is grafted with two different Eu^{3+}/Tb^{3+} ratios. $Tb_{0.5}Eu_{0.5}$@BpyDAT POP **44** is operative in the region 10 – 310 K, with a maximum sensitivity of 0.81 % K^{-1} (160 K). $Tb_{0.66}Eu_{0.34}$@BpyDAT POP showed temperature dependency in the 10 - 310 K, with a maximum sensitivity of 1.00 % K^{-1} (125 K). The temperature uncertainty is below 0.25 K for the region 60 – 310 K and the material revealed excellent repeatability of 98.5 %. The peculiar temperature behaviour, constant Tb^{3+} emission over the whole temperature range (as observed for the Eu^{3+}/Tb^{3+} grafted TpBpyCOF discussed above), is detected. The behaviour is explained through the same observations. First, the absence of ligand-to-Tb^{3+} energy back transfer is confirmed, since the triplet excited state energy of the ligand (24 040 cm^{-1}) lies well above the $^5D_0$ accepting level of Tb^{3+}. Second, electronic communication from Tb^{3+} to Eu^{3+} is limited as the conjugation in the material is interrupted at the aminal nodes, this is further proven by a constant decay time for Tb^{3+}. For future research, the investigation of fully conjugated frameworks is therefore recommended.

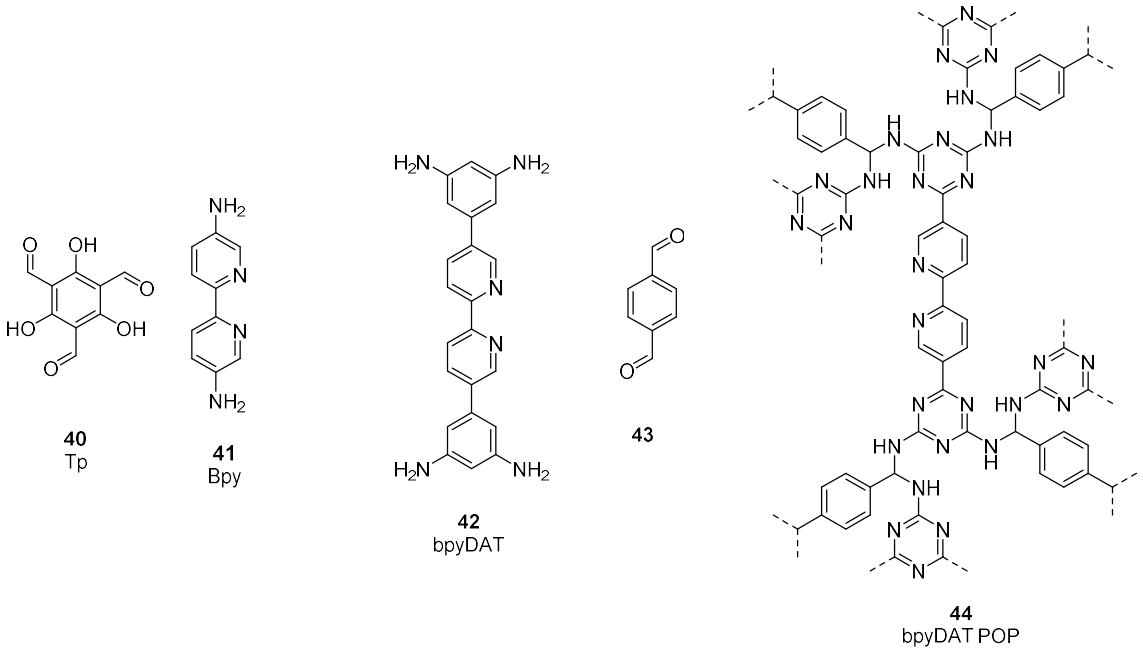

Figure 11. Building blocks of the reported COF and POP investigated for temperature sensing.

Conclusion and perspectives

The market share of noncontact temperature sensors is expending due to fast technological and medical evolutions. Lanthanide-based temperature sensors are the ideal thermometer candidate as they benefit from high photostability, relatively long decay times and high quantum yields. To circumvent their low molar light absorption, the incorporation of a light-harvesting antenna is required. This review presented the development of the N-rich lanthanide-based temperature sensors, emitting in the visible light spectrum. The N-rich antenna enables first, the formation of a Lewis adduct,

second, influences energy transfers through its triplet level and third, minimizes radiationless deactivation of the sensor. The N-rich ligands are incorporated in many different platforms. First, the molecular probes were discussed, containing a single trivalent lanthanide ion. Eu^{3+} is mostly reported and the corresponding sensors operate in the broad physiological range. The sensor based on Tb^{3+} is operational in a lower temperature range. Their application potential covers mainly temperature sensitive paints and intracellular temperature mapping, however, many systems have not been developed into applications. The path towards the final goal includes multiple obstacles (e.g. assessing bioavailability and toxicity), requiring an interdisciplinary approach. Second, the ratiometric temperature sensor is introduced, either as single- or dual-center, to cancel out influences from inhomogeneity in the material or the environment. Different N-rich platforms have been addressed. This review presents the investigation of N-rich antennae incorporated in polymers, MOFs, PMOs, and recently, in COFs and POPs. Overall, a very specific choice of lanthanide ratio provides the best result, testing and reporting of the multiple attempts are advised for a better understanding in the future. Generally, a higher amount of Tb^{3+} over Eu^{3+} was mostly reported. The antenna mainly determines the application potential of the ratiometric thermometer. Metal-organic-frameworks are generally very useful in the cryogenic region, periodic mesoporous organosilica show temperature dependency in the physiological range and porous organic polymers are operative in the cryogenic to medium temperature range. Formulating conclusions over and in the different types of materials explored for temperature sensing, remains hard. The outcome is namely influenced by different parameters and comparison could only be decisive if only one parameter was changed. The investigation of different platforms opens up opportunities of the sensors in different temperature regions, and coherently, in different applications. A more fundamental growth is expected in the novel research field of COFs as temperature sensor, while the more established researched platforms as MOFs will elaborate the application potential as thermometer. To improve and accelerate the global result, more coherence in the reported characteristics over the different research groups worldwide (especially the accessible information e.g. Tb^{3+}/Eu^{3+} ratios tested, triplet level antenna) is advised. The growth potential of lanthanide-based temperature sensors could also expand when the understanding on the energy transfer mechanisms is elaborated. As described in this review, the recently explored material categories COFs and POPs show peculiar temperature behaviour due to modified energy transfer mechanisms. Further investigation of other COFs and POPs would therefore be required to observe a possible trend in the reported peculiar behaviour. Moreover, the synthesis of a single crystal COF could allow precise determination of the location of Tb^{3+} and Eu^{3+} ions in the framework. In this way, the distance between the different ion centers could be unravelled and further investigation of the proposed energy transfer mechanisms could be investigated. Gaining insight into the nature and main features of energy transfer mechanisms is essential to predict materials with low energy loss and high radiation efficiency. The research should therefore go beyond the experimental obtained results. However, it should be mentioned here that understanding and predicting energy transfer thermometry is far from a trivial task. Only recently the first theoretical framework for ratiometric single ion luminescent thermometry has been laid.[98] We hope that further work on more complex to study energy transfer thermometry will also be reported soon. Some computational studies have been conducted for mononuclear and dinuclear lanthanide complexes of Eu^{3+} and Tb^{3+} ions.[99-100] However, MOFs, PMOs, COFs and POPs contain multiple ligands and lanthanide ions, therefore, the modelled energy transfers for a single complex must be extended towards the developed mixture of active centres in the framework. In this way, the combination of theoretical and experimental input could provide insights in the energy transfer mechanisms. Furthermore, computational studies allow more efficient and targeted experimental development of novel antennae. The energy gap between the lowest triplet level of the ligand and the emitting level of the lanthanide ion is key in determining the luminescence performance. Through computational studies, the excited states can be localized and

10.1002/chem.202100007

the triplet level of novel antennae can be calculated, in this way, the influence of for example different substituents on the triplet level of different antennae are investigated. The experimental results of the performance of the temperature sensor therefore provide input for advanced modelling studies, creating a smart methodology for the future development of temperature sensors.

References

1. L. Michalski, K. E., J. Kucharski, J. McGhee, Author and Organisation Index. In *Temperature Measurement*, John Wiley & Sons Ltd: West Sussex, England, 2002; pp 471-478.
2. Benedict, R. P., *Fundamentals of Temperature, Pressure and Flow Measurements*. John Wiley & Sons Ltd: New York, 1977.
3. Childs, P. R. N.; Greenwood, J. R.; Long, C. A., Review of temperature measurement. *Review of Scientific Instruments* **2000,** *71* (8), 2959-2978.
4. Khalid, A. H. K., K., Thermographic Phosphors for High Temperature Measurements: Principles, Current State of the Art and Recent Applications. *Sensors* **2008,** *8* (9), 5673-5744.
5. McCabe, K. M.; Hernandez, M., Molecular thermometry. *Pediatric research* **2010,** *67* (5), 469-75.
6. Jaque, D.; Vetrone, F., Luminescence nanothermometry. *Nanoscale* **2012,** *4* (15), 4301-4326.
7. Uchiyama, S.; Gota, C.; Tsuji, T.; Inada, N., Intracellular temperature measurements with fluorescent polymeric thermometers. *Chemical Communications* **2017,** *53* (80), 10976-10992.
8. *Temperate sensor market, global forecast to 2027 (by product type, output, end-user industry, and geography)*; SE 2914; Markets and Markets: 2020.
9. Brites, C. D. S.; Millán, A.; Carlos, L. D., Chapter 281 - Lanthanides in Luminescent Thermometry. In *Handbook on the Physics and Chemistry of Rare Earths*, Jean-Claude, B.; Vitalij K, P., Eds. Elsevier: 2016; Vol. 49, pp 339-427.
10. Ferreira, R. A.; Brites, C. D. S.; Vicente, C. M.; Lima, P. P.; Bastos, A. R.; Marques, P. G.; Hiltunen, M.; Carlos, L. D.; André, P. S., Photonic-on-a-chip: a thermal actuated Mach-Zehnder interferometer and a molecular thermometer based on a single di-ureasil organic-inorganic hybrid. *Laser & Photonics Reviews* **2013,** *7* (6), 1027-1035.
11. He, R.; de Aldana, J. R. V.; Pedrola, G. L.; Chen, F.; Jaque, D., Two-photon luminescence thermometry: towards 3D high-resolution thermal imaging of waveguides. *Optics Express* **2016,** *24* (14), 16156-16166.
12. Brites, C.; Pereira, P.; João, N.; Millán, A.; Amaral, V.; Palacio, F.; Carlos, L. A. D., Organic–Inorganic Eu3+/Tb3+ codoped hybrid films for temperature mapping in integrated circuits. *Frontiers in chemistry* **2013,** *1*, 9.
13. Savchuk, O. A.; Carvajal, J.; Massons, J.; Cascales, C.; Aguiló, M.; Díaz, F., Novel low-cost, compact and fast signal processing sensor for ratiometric luminescent nanothermometry. *Sensors and Actuators A: Physical* **2016,** *250*, 87-95.
14. Geitenbeek, R. G.; Nieuwelink, A.-E.; Jacobs, T. S.; Salzmann, B. B.; Goetze, J.; Meijerink, A.; Weckhuysen, B. M., In situ luminescence thermometry to locally measure temperature gradients during catalytic reactions. *ACS catalysis* **2018,** *8* (3), 2397-2401.
15. Abram, C.; Fond, B.; Beyrau, F., Temperature measurement techniques for gas and liquid flows using thermographic phosphor tracer particles. *Progress in energy and combustion science* **2018,** *64*, 93-156.
16. Miyagawa, T.; Fujie, T.; Ferdinandus; Vo Doan, T. T.; Sato, H.; Takeoka, S., Glue-Free Stacked Luminescent Nanosheets Enable High-Resolution Ratiometric Temperature Mapping in Living Small Animals. *ACS Applied Materials & Interfaces* **2016,** *8* (49), 33377-33385.
17. Ferdinandus; Arai, S.; Takeoka, S.; Ishiwata, S. i.; Suzuki, M.; Sato, H., Facilely Fabricated Luminescent Nanoparticle Thermosensor for Real-Time Microthermography in Living Animals. *ACS Sensors* **2016,** *1* (10), 1222-1227.

18. Piñol, R.; Brites, C. D. S.; Silva, N. J.; Carlos, L. D.; Millán, A., Chapter 6 - Nanoscale Thermometry for Hyperthermia Applications. In *Nanomaterials for Magnetic and Optical Hyperthermia Applications*, Fratila, R. M.; De La Fuente, J. M., Eds. Elsevier: 2019; pp 139-172.
19. Savchuk, O. A.; Silvestre, O. F.; Adão, R. M. R.; Nieder, J. B., GFP fluorescence peak fraction analysis based nanothermometer for the assessment of exothermal mitochondria activity in live cells. *Scientific Reports* **2019,** *9* (1), 7535.
20. Mateos, S.; Lifante, J.; Li, C.; Ximendes, E. C.; Muñoz-Ortiz, T.; Yao, J.; de la Fuente-Fernández, M.; García Villalón, Á. L.; Granado, M.; Zabala Gutierrez, I., Instantaneous In Vivo Imaging of Acute Myocardial Infarct by NIR-II Luminescent Nanodots. *Small* **2020**, 1907171.
21. Santos, H. D.; Ximendes, E. C.; Iglesias-de la Cruz, M. d. C.; Chaves-Coira, I.; del Rosal, B.; Jacinto, C.; Monge, L.; Rubia-Rodríguez, I.; Ortega, D.; Mateos, S., In vivo early tumor detection and diagnosis by infrared luminescence transient nanothermometry. *Advanced Functional Materials* **2018,** *28* (43), 1803924.
22. Brites, C. D.; Lima, P. P.; Silva, N. J.; Millán, A.; Amaral, V. S.; Palacio, F.; Carlos, L. D., Thermometry at the nanoscale. *Nanoscale* **2012,** *4* (16), 4799-4829.
23. Brites, C. D. S.; Balabhadra, S.; Carlos, L. D., Lanthanide-Based Thermometers: At the Cutting-Edge of Luminescence Thermometry. *Advanced Optical Materials* **2019,** *7* (5), 1801239.
24. Cho, S. J.; Maysinger, D.; Jain, M.; Röder, B.; Hackbarth, S.; Winnik, F. M., Long-term exposure to CdTe quantum dots causes functional impairments in live cells. *Langmuir : the ACS journal of surfaces and colloids* **2007,** *23* (4), 1974-80.
25. Gnach, A.; Lipinski, T.; Bednarkiewicz, A.; Rybka, J.; Capobianco, J. A., Upconverting nanoparticles: assessing the toxicity. *Chemical Society Reviews* **2015,** *44* (6), 1561-1584.
26. Bünzli, J.-C. G., Benefiting from the unique properties of lanthanide ions. *Accounts of chemical research* **2006,** *39* (1), 53-61.
27. Bünzli, J.-C. G.; Piguet, C., Taking advantage of luminescent lanthanide ions. *Chemical Society Reviews* **2005,** *34* (12), 1048-1077.
28. Sahu, P. C.; Nagar Venkataraman, C. S., Actinide and Lanthanide Systems, High Pressure Behavior. In *Encyclopedia of Metalloproteins*, Kretsinger, R. H.; Uversky, V. N.; Permyakov, E. A., Eds. Springer New York: New York, NY, 2013; pp 5-11.
29. Carlos, L.; Ferreira, R., V. d. Z. Bermudez and SJL Ribeiro. *Adv. Mater* **2009,** *21* (5), 509-534.
30. Binnemans, K., Lanthanide-based luminescent hybrid materials. *Chem Rev* **2009,** *109* (9), 4283-374.
31. Bünzli, J.-C. G., On the design of highly luminescent lanthanide complexes. *Coordination Chemistry Reviews* **2015,** *293-294*, 19-47.
32. Hasegawa, Y.; Kitagawa, Y., Thermo-sensitive luminescence of lanthanide complexes, clusters, coordination polymers and metal–organic frameworks with organic photosensitizers. *Journal of Materials Chemistry C* **2019,** *7* (25), 7494-7511.
33. Tsaryuk, V.; Vologzhanina, A.; Zhuravlev, K.; Kudryashova, V., Structures and optical spectroscopy of lanthanide trifluoroacetates obtained from hexafluoroacetylacetone. *Journal of Fluorine Chemistry* **2017,** *197*, 87-93.
34. Katagiri, S.; Tsukahara, Y.; Hasegawa, Y.; Wada, Y., Energy-transfer mechanism in photoluminescent terbium (III) complexes causing their temperature-dependence. *Bulletin of the Chemical Society of Japan* **2007,** *80* (8), 1492-1503.

35. Weissman, S., Intramolecular energy transfer the fluorescence of complexes of europium. *The Journal of Chemical Physics* **1942,** *10* (4), 214-217.
36. Bhaumik, M., Quenching and Temperature Dependence of Fluorescence in Rare-Earth Chelates. *The Journal of Chemical Physics* **1964,** *40* (12), 3711-3715.
37. Ohlmann, R. C.; Charles, R. G., Fluorescence Properties of Europium Dibenzoylmethide and Its Complexes with Lewis Bases. *The Journal of Chemical Physics* **1964,** *40* (10), 3131-3133.
38. Sato, S.; Ishii, A.; Yamada, C.; Kim, J.; Ho Song, C.; Fujiwara, A.; Takata, M.; Hasegawa, M., Luminescence of fusion materials of polymeric chain-structured lanthanide complexes. *Polymer Journal* **2015,** *47* (2), 195-200.
39. Khalil, G. E.; Lau, K.; Phelan, G. D.; Carlson, B.; Gouterman, M.; Callis, J. B.; Dalton, L. R., Europium beta-diketonate temperature sensors: Effects of ligands, matrix, and concentration. *Review of Scientific Instruments* **2004,** *75* (1), 192-206.
40. Ogle, M. M.; Smith McWilliams, A. D.; Jiang, B.; Martí, A. A., Latest Trends in Temperature Sensing by Molecular Probes. *ChemPhotoChem* **2020**.
41. Rocha, J.; Brites, C. D.; Carlos, L. D., Lanthanide organic framework luminescent thermometers. *Chemistry–A European Journal* **2016,** *22* (42), 14782-14795.
42. Kaczmarek, A. M.; Van Der Voort, P., Light-Emitting Lanthanide Periodic Mesoporous Organosilica (PMO) Hybrid Materials. *Materials (Basel, Switzerland)* **2020,** *13* (3).
43. Zhang, Y.; Yuan, S.; Day, G.; Wang, X.; Yang, X.; Zhou, H.-C., Luminescent sensors based on metal-organic frameworks. *Coordination Chemistry Reviews* **2018,** *354*, 28-45.
44. Lustig, W. P.; Mukherjee, S.; Rudd, N. D.; Desai, A. V.; Li, J.; Ghosh, S. K., Metal–organic frameworks: functional luminescent and photonic materials for sensing applications. *Chemical Society Reviews* **2017,** *46* (11), 3242-3285.
45. Cui, Y.; Zhu, F.; Chen, B.; Qian, G., Metal–organic frameworks for luminescence thermometry. *Chemical Communications* **2015,** *51* (35), 7420-7431.
46. Cui, Y.; Zhang, J.; He, H.; Qian, G., Photonic functional metal–organic frameworks. *Chemical Society Reviews* **2018,** *47* (15), 5740-5785.
47. Haug, W. K.; Moscarello, E. M.; Wolfson, E. R.; McGrier, P. L., The luminescent and photophysical properties of covalent organic frameworks. *Chemical Society Reviews* **2020,** *49* (3), 839-864.
48. Wang, X.-d.; Wolfbeis, O. S.; Meier, R. J., Luminescent probes and sensors for temperature. *Chemical Society Reviews* **2013,** *42* (19), 7834-7869.
49. Borisov, S. M.; Wolfbeis, O. S., Temperature-Sensitive Europium(III) Probes and Their Use for Simultaneous Luminescent Sensing of Temperature and Oxygen. *Analytical Chemistry* **2006,** *78* (14), 5094-5101.
50. Zelelow, B.; Khalil, G. E.; Phelan, G.; Carlson, B.; Gouterman, M.; Callis, J. B.; Dalton, L. R., Dual luminophor pressure sensitive paint: II. Lifetime based measurement of pressure and temperature. *Sensors and Actuators B: Chemical* **2003,** *96* (1), 304-314.
51. Mitsuishi, M.; Kikuchi, S.; Miyashita, T.; Amao, Y., Characterization of an ultrathin polymer optode and its application to temperature sensors based on luminescent europium complexes. *Journal of Materials Chemistry* **2003,** *13* (12), 2875-2879.
52. Stich, M. I. J.; Nagl, S.; Wolfbeis, O. S.; Henne, U.; Schaeferling, M., A Dual Luminescent Sensor Material for Simultaneous Imaging of Pressure and Temperature on Surfaces. *Advanced Functional Materials* **2008,** *18* (9), 1399-1406.

53. Yu, J.; Sun, L.; Peng, H.; Stich, M. I. J., Luminescent terbium and europium probes for lifetime based sensing of temperature between 0 and 70 °C. *Journal of Materials Chemistry* **2010,** *20* (33), 6975-6981.
54. Lapaev, D. V.; Nikiforov, V. G.; Lobkov, V. S.; Knyazev, A. A.; Ziyatdinova, R. M.; Galyametdinov, Y. G., A vitrified film of an anisometric europium(iii) β-diketonate complex with a low melting point as a reusable luminescent temperature probe with excellent sensitivity in the range of 270–370 K. *Journal of Materials Chemistry C* **2020**.
55. Lapaev, D. V.; Nikiforov, V. G.; Lobkov, V. S.; Knyazev, A. A.; Galyametdinov, Y. G., Reusable temperature-sensitive luminescent material based on vitrified film of europium(III) β-diketonate complex. *Optical Materials* **2018,** *75*, 787-795.
56. Knyazev, A. A.; Krupin, A. S.; Molostova, E. Y.; Romanova, K. A.; Galyametdinov, Y. G., Influence of Structural Anisotropy on Mesogenity of Eu(III) Adducts and Optical Properties of Vitrified Films Formed on their Base. *Inorganic Chemistry* **2015,** *54* (18), 8987-8993.
57. Kolodner, P.; Tyson, J. A., Remote thermal imaging with 0.7-μm spatial resolution using temperature-dependent fluorescent thin flims. *Applied Physics Letters* **1983,** *42* (1), 117-119.
58. Hasegawa, Y.; Murakoshi, K.; Wada, Y.; Yanagida, S.; Kim, J.-H.; Nakashima, N.; Yamanaka, T., Enhancement of luminescence of Nd3+ complexes with deuterated hexafluoroacetylacetonato ligands in organic solvent. *Chemical Physics Letters* **1996,** *248* (1), 8-12.
59. Berry, M. T.; May, P. S.; Xu, H., Temperature Dependence of the Eu3+ 5D0 Lifetime in Europium Tris(2,2,6,6-tetramethyl-3,5-heptanedionato). *The Journal of Physical Chemistry* **1996,** *100* (22), 9216-9222.
60. Lapaev, D. V.; Nikiforov, V. G.; Lobkov, V. S.; Knyazev, A. A.; Galyametdinov, Y. G., A photostable vitrified film based on a terbium(iii) β-diketonate complex as a sensing element for reusable luminescent thermometers. *Journal of Materials Chemistry C* **2018,** *6* (35), 9475-9481.
61. Kitos, A. A.; Gálico, D. A.; Castañeda, R.; Ovens, J. S.; Murugesu, M.; Brusso, J. L., Stark Sublevel-Based Thermometry with Tb(III) and Dy(III) Complexes Cosensitized via the 2-Amidinopyridine Ligand. *Inorganic Chemistry* **2020,** *59* (15), 11061-11070.
62. Wang, X.-d.; Song, X.-h.; He, C.-y.; Yang, C. J.; Chen, G.; Chen, X., Preparation of Reversible Colorimetric Temperature Nanosensors and Their Application in Quantitative Two-Dimensional Thermo-Imaging. *Analytical Chemistry* **2011,** *83* (7), 2434-2437.
63. Lu, S.; Sun, J.; Wang, Y.; Yu, W.; Sun, M.; Cui, S., Preparation and properties of temperature sensitive paint based on Eu(DBM)3phen as probe molecule. *Journal of Rare Earths* **2018,** *36* (6), 669-674.
64. Swavey, S.; Krause, J. A.; Collins, D.; D'Cunha, D.; Fratini, A., X-ray structure and temperature dependent luminescent properties of two bimetallic europium complexes. *Polyhedron* **2008,** *27* (3), 1061-1069.
65. Gálico, D. A.; Marin, R.; Brunet, G.; Errulat, D.; Hemmer, E.; Sigoli, F. A.; Moilanen, J. O.; Murugesu, M., Triplet-State Position and Crystal-Field Tuning in Opto-Magnetic Lanthanide Complexes: Two Sides of the Same Coin. *Chemistry – A European Journal* **2019,** *25* (64), 14625-14637.
66. Guo, X.-Q.; Zhou, L.-P.; Cai, L.-X.; Sun, Q.-F., Self-Assembled Bright Luminescent Lanthanide-Organic Polyhedra for Ratiometric Temperature Sensing. *Chemistry – A European Journal* **2018,** *24* (27), 6936-6940.

67. Bao, G.; Wong, K.-L.; Jin, D.; Tanner, P. A., A stoichiometric terbium-europium dyad molecular thermometer: energy transfer properties. *Light: Science & Applications* **2018,** *7* (1), 96.
68. Yang, D.; Liu, D.; Tian, C.; Wang, S.; Li, H., Flexible and transparent films consisting of lanthanide complexes for ratiometric luminescence thermometry. *Journal of colloid and interface science* **2018,** *519*, 11-17.
69. Zhou, X.; Wang, H.; Jiang, S.; Xiang, G.; Tang, X.; Luo, X.; Li, L.; Zhou, X., Multifunctional Luminescent Material Eu(III) and Tb(III) Complexes with Pyridine-3,5-Dicarboxylic Acid Linker: Crystal Structures, Tunable Emission, Energy Transfer, and Temperature Sensing. *Inorganic Chemistry* **2019,** *58* (6), 3780-3788.
70. Vanden Bussche, F.; Kaczmarek, A. M.; Schmidt, J.; Stevens, C. V.; Van Der Voort, P., Lanthanide grafted phenanthroline-polymer for physiological temperature range sensing. *Journal of Materials Chemistry C* **2019,** *7* (35), 10972-10980.
71. Liu, W.; Chen, C.; Huang, X.; Xie, E.; Liu, W., Functional Construction of Dual-Emitting 4-Aminonaphthalimide Encapsulated Lanthanide MOFs Composite for Ratiometric Temperature Sensing. *Chemistry – A European Journal* **2019,** *25* (43), 10054-10058.
72. Cui, Y.; Xu, H.; Yue, Y.; Guo, Z.; Yu, J.; Chen, Z.; Gao, J.; Yang, Y.; Qian, G.; Chen, B., A Luminescent Mixed-Lanthanide Metal–Organic Framework Thermometer. *Journal of the American Chemical Society* **2012,** *134* (9), 3979-3982.
73. Rao, X.; Song, T.; Gao, J.; Cui, Y.; Yang, Y.; Wu, C.; Chen, B.; Qian, G., A Highly Sensitive Mixed Lanthanide Metal–Organic Framework Self-Calibrated Luminescent Thermometer. *Journal of the American Chemical Society* **2013,** *135* (41), 15559-15564.
74. Cui, Y.; Zou, W.; Song, R.; Yu, J.; Zhang, W.; Yang, Y.; Qian, G., A ratiometric and colorimetric luminescent thermometer over a wide temperature range based on a lanthanide coordination polymer. *Chemical Communications* **2014,** *50* (6), 719-721.
75. Wu, L.-L.; Zhao, J.; Wang, H.; Wang, J., A lanthanide(iii) metal–organic framework exhibiting ratiometric luminescent temperature sensing and tunable white light emission. *CrystEngComm* **2016,** *18* (23), 4268-4271.
76. Zhou, Y.; Yan, B.; Lei, F., Postsynthetic lanthanide functionalization of nanosized metal–organic frameworks for highly sensitive ratiometric luminescent thermometry. *Chemical Communications* **2014,** *50* (96), 15235-15238.
77. Zhou, Y.; Yan, B., Lanthanides post-functionalized nanocrystalline metal–organic frameworks for tunable white-light emission and orthogonal multi-readout thermometry. *Nanoscale* **2015,** *7* (9), 4063-4069.
78. Kaczmarek, A. M.; Liu, Y.-Y.; Wang, C.; Laforce, B.; Vincze, L.; Van Der Voort, P.; Van Deun, R., Grafting of a Eu3+-tfac complex on to a Tb3+-metal organic framework for use as a ratiometric thermometer. *Dalton Transactions* **2017,** *46* (37), 12717-12723.
79. Kaczmarek, A. M.; Liu, Y.-Y.; Wang, C.; Laforce, B.; Vincze, L.; Van Der Voort, P.; Van Hecke, K.; Van Deun, R., Lanthanide "Chameleon" Multistage Anti-Counterfeit Materials. *Advanced Functional Materials* **2017,** *27* (20), 1700258.
80. Zhao, S.-N.; Li, L.-J.; Song, X.-Z.; Zhu, M.; Hao, Z.-M.; Meng, X.; Wu, L.-L.; Feng, J.; Song, S.-Y.; Wang, C.; Zhang, H.-J., Lanthanide Ion Codoped Emitters for Tailoring Emission Trajectory and Temperature Sensing. *Advanced Functional Materials* **2015,** *25* (9), 1463-1469.
81. Zhao, D.; Wang, H.; Qian, G., Synthesis, structure and temperature sensing of a lanthanide-organic framework constructed from a pyridine-containing tetracarboxylic acid ligand. *CrystEngComm* **2018,** *20* (45), 7395-7400.

82. Feng, X.; Shang, Y.; Zhang, H.; Liu, X.; Wang, X.; Chen, N.; Wang, L.; Li, Z., Multi-functional lanthanide-CPs based on tricarboxylphenyl terpyridyl ligand as ratiometric luminescent thermometer and highly sensitive ion sensor with turn on/off effect. *Dalton Transactions* **2020,** *49* (15), 4741-4750.
83. Wei, Y.; Sa, R.; Li, Q.; Wu, K., Highly stable and sensitive LnMOF ratiometric thermometers constructed with mixed ligands. *Dalton Transactions* **2015,** *44* (7), 3067-3074.
84. Shen, X.; Lu, Y.; Yan, B., Lanthanide Complex Hybrid System for Fluorescent Sensing as Thermometer. *European Journal of Inorganic Chemistry* **2015,** *2015* (6), 916-919.
85. Han, Y.-H.; Tian, C.-B.; Li, Q.-H.; Du, S.-W., Highly chemical and thermally stable luminescent EuxTb1−x MOF materials for broad-range pH and temperature sensors. *Journal of Materials Chemistry C* **2014,** *2* (38), 8065-8070.
86. An, R.; Zhao, H.; Hu, H.-M.; Wang, X.; Yang, M.-L.; Xue, G., Synthesis, Structure, White-Light Emission, and Temperature Recognition Properties of Eu/Tb Mixed Coordination Polymers. *Inorganic Chemistry* **2016,** *55* (2), 871-876.
87. Zaręba, J. K.; Nyk, M.; Janczak, J.; Samoć, M., Three-Photon Absorption of Coordination Polymer Transforms UV-to-VIS Thermometry into NIR-to-VIS Thermometry. *ACS Applied Materials & Interfaces* **2019,** *11* (11), 10435-10441.
88. Yang, Y.; Huang, H.; Wang, Y.; Qiu, F.; Feng, Y.; Song, X.; Tang, X.; Zhang, G.; Liu, W., A family of mixed-lanthanide metal–organic framework thermometers in a wide temperature range. *Dalton Transactions* **2018,** *47* (38), 13384-13390.
89. Liu, X.; Akerboom, S.; Jong, M. d.; Mutikainen, I.; Tanase, S.; Meijerink, A.; Bouwman, E., Mixed-Lanthanoid Metal–Organic Framework for Ratiometric Cryogenic Temperature Sensing. *Inorganic Chemistry* **2015,** *54* (23), 11323-11329.
90. Quintanilla, M.; Liz-Marzán, L. M., Guiding Rules for Selecting a Nanothermometer. *Nano Today* **2018,** *19*, 126-145.
91. Kaczmarek, A. M.; Van Deun, R.; Van Der Voort, P., Nanothermometers based on lanthanide incorporated Periodic Mesoporous Organosilica. *Journal of Materials Chemistry C* **2019,** *7* (14), 4222-4229.
92. Bourda, L.; Jena, H. S.; Van Deun, R.; Kaczmarek, Anna M.; Van Der Voort, P., Functionalized periodic mesoporous organosilicas: from metal free catalysis to sensing. *Journal of Materials Chemistry A* **2019,** *7* (23), 14060-14069.
93. Kaczmarek, A. M.; Maegawa, Y.; Abalymov, A.; Skirtach, A. G.; Inagaki, S.; Van Der Voort, P., Lanthanide-Grafted Bipyridine Periodic Mesoporous Organosilicas (BPy-PMOs) for Physiological Range and Wide Temperature Range Luminescence Thermometry. *ACS Applied Materials & Interfaces* **2020,** *12* (11), 13540-13550.
94. Kaczmarek, A. M.; Esquivel, D.; Laforce, B.; Vincze, L.; Van Der Voort, P.; Romero-Salguero, F. J.; Van Deun, R., Luminescent thermometer based on Eu3+/Tb3+-organic-functionalized mesoporous silica. *Luminescence* **2018,** *33* (3), 567-573.
95. Kaczmarek, A. M.; Esquivel, D.; Ouwehand, J.; Van Der Voort, P.; Romero-Salguero, F. J.; Van Deun, R., Temperature dependent NIR emitting lanthanide-PMO/silica hybrid materials. *Dalton Transactions* **2017,** *46* (24), 7878-7887.
96. Kaczmarek, A. M.; Liu, Y.-Y.; Kaczmarek, M. K.; Liu, H.; Artizzu, F.; Carlos, L. D.; Van Der Voort, P., Developing Luminescent Ratiometric Thermometers Based on a Covalent Organic Framework (COF). *Angewandte Chemie International Edition* **2020,** *59* (5), 1932-1940.
97. Dieke, G. H.; Crosswhite, H. M.; Crosswhite, H., Spectra and energy levels of rare earth ions in crystals. **1968**.

98. Suta, M.; Meijerink, A., A Theoretical Framework for Ratiometric Single Ion Luminescent Thermometers—Thermodynamic and Kinetic Guidelines for Optimized Performance. *Advanced Theory and Simulations* **2020,** *3* (12), 2000176.
99. Romanova, K. A.; Freidzon, A. Y.; Bagaturyants, A. A.; Galyametdinov, Y. G., Ab Initio Study of Energy Transfer Pathways in Dinuclear Lanthanide Complex of Europium(III) and Terbium(III) Ions. *The Journal of Physical Chemistry A* **2014,** *118* (47), 11244-11252.
100. Yu, Z.; Shen, L.; Li, D.; Pun, E. Y. B.; Zhao, X.; Lin, H., Fluctuation of photon-releasing with ligand coordination in polyacrylonitrile-based electrospun nanofibers. *Scientific Reports* **2020,** *10* (1), 926.

Graphical Abstract

The overview of N-rich antennae investigated in lanthanide-based temperature sensing

Flore Vanden Bussche, Anna M. Kaczmarek, Veronique Van Speybroeck, Pascal Van Der Voort, Christian V. Stevens[a]